Elrayah
*Journal of Engineering and Applied Science* (2024) 71:86
https://doi.org/10.1186/s44147-024-00383-0

Journal of Engineering and Applied Science

**RESEARCH** **Open Access**

# Enhancing drilling operations: prioritizing wellbore integrity, formation preservation, and effective mud waste control (case study)

Ahmed Abdelaziz Ibrahim Elrayah[1*]

*Correspondence:
ahtasaspe@gmail.com;
ahmedabdelaziz@sustech.edu

[1] College of Petroleum and Mining Engineering, Petroleum Engineering Department, Sudan University of Science and Technology, Khartoum, Sudan

## Abstract

This study examined the issues of wellbore instability encountered during the drilling of the vertical exploration Al-Rateena-1 well, Block 25D, Al-Rawat Field, Sudan. Measurements of the wellbore diameter revealed significant damage to the formation interval between 2775 and 2925 m. This damage released approximately 800 barrels of drill cuttings from the affected zone and overlying formations. A comprehensive wellbore stability assessment was conducted to identify the root causes of instability and develop strategies to mitigate future occurrences. The assessment involved a thorough analysis of the pore, vertical, effective vertical, and minimum and maximum horizontal pressures. All of these parameters play a crucial role in maintaining wellbore integrity. This study also evaluated the potential impact of these parameters on groundwater and soil quality, leading to the development of an efficient waste management system. The safe mud weight range for the well was determined to be between 13.5 and 15.5 pounds per gallon (PPG). However, the drilling fluid used during the operation had a significantly lower density of only 10 PPG. This ultimately leads to the collapse of the wellbore wall. Examination of drilling cuttings revealed elevated levels of various heavy metals. These heavy metals included Lead (94.12 ppm), Mercury (62.87 ppm), Nickel (1403 ppm), Copper (343 ppm), Calcium (23132.72 ppm), Magnesium (3700 ppm), and Barium (16000 ppm). These elements pose a significant threat to both surface water and groundwater quality. It is possible that they also contributed to the wellbore wall collapse. It was hypothesized that the interaction between these elements and the water-based drilling fluid or its additives could have triggered the collapse event. The findings of this study highlight the importance of conducting comprehensive wellbore stability assessments before drilling. Such assessments should incorporate detailed investigations, modelling, calculations, and simulations of various parameters that influence wellbore stability. In addition, careful consideration must be given to the potential environmental impacts of drilling fluids and cuttings, particularly in areas with sensitive ecosystems. The wellbore instability in the vertical exploration Al-Rateena-1 well was primarily caused by the use of an underweight drilling fluid. This underweight drilling fluid results in the collapse of the wellbore wall. Elevated levels of heavy metals in drill cuttings suggest a potential impact on groundwater quality. It is also possible that they contributed to the wellbore instability. Comprehensive wellbore stability assessments are essential to prevent similar incidents in the future. This study provides a detailed account of wellbore instability. This includes the identification of root causes and the development of preventive measures. This study also highlights the potential environmental impact of drilling fluids and cuttings. The findings of this study can help improve drilling practices and environmental protection in the oil and gas industry.

**Keywords:** Formation damage, Geomechanical pressure, Mud waste control, Wellbore integrity, Wellbore stability

## Introduction

Maintaining wellbore integrity and minimizing formation impairment are paramount in oil and gas exploration, given the dynamic industrial landscape and the complexities of extracting subsurface energy resources. The complex interplay of physical and chemical factors necessitates a forward-looking approach to mitigate these challenges. However, overbalanced drilling can lead to mechanical complications, potentially necessitating remedial intervention or good abandonment. Formation damage, which is influenced by mechanical, chemical, biological, and thermal factors, can hinder production. Maintaining wellbore stability and minimizing formation damage are paramount concerns in the perpetually dynamic landscape of oil and gas exploration. These aspects are intrinsically linked to the complexities of extracting concealed energy resources, which required a proactive strategy to address them. However, excessive drilling pressure can cause mechanical complications that may necessitate further intervention, even well abandonment. Furthermore, formation damage; resulting from a confluence of mechanical, chemical, biological, and thermal factors, can hinder production output [1–6].

The oil and gas industry generates a significant amount of waste, including drilling cuttings, which may contain harmful chemicals. Improper handling of these cuttings poses environmental risks because they can contaminate soils and sediments. Heavy metals, such as cadmium, lead, chromium, and arsenic; are often present in drilling cuttings because of their use as drilling fluids and additives. These metals can accumulate in soils and sediments, posing a threat to aquatic organisms and potentially entering the food chain. The soil is a vital interface between human activities and the environment, and its protection is crucial for maintaining a healthy ecosystem. However, increasing industrialization and urbanization have led to the release of heavy metals into the environment through exploration and extraction operations. This highlights the need for effective waste management practices in the oil and gas industry to minimize environmental contamination and protect human health. Regular monitoring of heavy metal concentrations in soils near drilling sites is crucial for identifying potential contamination hotspots and implementing appropriate remediation measures. Proper treatment and disposal of drilling cuttings are essential to prevent the release of heavy metals into the environment. Public awareness campaigns can inform local communities about the potential risks associated with oil and gas drilling activities and encourage protective measures [7–10].

Potential risks include polycyclic aromatic hydrocarbons (PAHs), a group of organic compounds formed during the incomplete combustion of organic matter. They are found in drilling cuttings because of their presence in crude oil and other petroleum products. PAHs are carcinogenic and can cause other health problems, including reproductive and developmental problems. Studies have shown that PAHs are present in drilling cuttings, sediments, soils, and vegetation in oil-producing regions. These studies have also shown that PAHs pose health risks to humans and wildlife. Effective waste management practices and environmental monitoring are required to minimize PAH contamination and protect human health [11–13].

Total Petroleum Hydrocarbons (TPHs) are another group of hydrocarbons found in crude oil and other petroleum products and pose significant environmental risks due to their potential adverse effects on soil, water, and human health. Researchers have developed various methods to measure TPH concentrations in soil, including gas chromatography/flame ionization detection (GC/FID). Cleanup procedures are often employed to remove naturally occurring organics that can interfere with TPH analysis. Studies investigating TPH contamination in the Niger Delta, a critical wetland ecosystem, have revealed high levels of TPH, heavy metals, and nutrients, particularly during the wet season. These findings underscore the urgent need for improved pollution control measures to address the environmental challenges posed by oil exploitation and global changes in the region [14–16].

Organochlorine pesticides (OCPs), a class of persistent organic pollutants (POPs), are widely used in agriculture and public health. However, their effectiveness in pest control has resulted in steep environmental costs. OCPs exhibit remarkable persistence in the environment and accumulate in soil and sediments over time. This persistence, coupled with their tendency to bioaccumulate in organisms, has led to widespread contamination of ecosystems worldwide. The African continent faces a unique challenge in addressing OCP contamination. Despite being banned in many developed countries, OCPs remain widely used in Africa, primarily for vector control in malaria prevention. This continued use has resulted in elevated levels of OCP residues in the African environment, posing significant risks to human and ecological health. The pervasive presence of OCPs in Africa has raised concerns regarding their potential adverse effects on human health. Studies have linked OCP exposure to a range of health issues, including developmental problems in children, reproductive disorders, and increased risk of certain cancers. Contamination of breast milk with OCPs poses a particular threat to infants and young children as they are particularly susceptible to the toxic effects of these compounds. Ecologically, OCP contamination has detrimental effects on various organisms, including fish, birds, and other beneficial insects. These contaminants disrupt ecosystems, affect biodiversity, and reduce agricultural productivity. However, the long-term effects of OCP contamination on African ecosystems remain largely unknown, highlighting the need for further research. Addressing the OCP contamination crisis in Africa requires a multipronged approach. The implementation of effective pesticide management strategies, including the promotion of safer alternatives to OCPs, is crucial. Raising awareness among farmers and domestic users about the proper handling and disposal of pesticides is essential for reducing OCP usage and preventing further environmental contamination. Moreover, strengthening regulatory frameworks and enforcing existing bans on OCPs are critical steps toward reducing their use. In addition, research efforts should focus on developing sensitive analytical methods for detecting OCPs and their metabolites to improve the understanding of the extent of contamination and its health and ecological impacts. OCP contamination poses a significant threat to environmental and public health in Africa. Despite the ban in many countries, the continued use of these persistent pesticides highlights the need for urgent action. Implementing effective pesticide management strategies, strengthening regulatory frameworks, and conducting further research are essential steps toward mitigating OCP contamination and protecting human and ecological health in Africa [17–19].

Biocides are chemical substances used to control microbial growth in various applications, including drilling fluids, hydraulic fracturing, and disinfectants. Although effective in controlling microbial growth, biocides can also pose risks to the environment and human health. Biocides are employed in drilling fluids to prevent the growth of microorganisms, which can lead to corrosion, souring, and plugging. However, some biocides can be toxic to aquatic organisms and disrupt soil ecosystems. Hydraulic fracturing operations use biocides to control microbial growth in the produced and flowback waters. This water has the potential to contaminate surface aquifers and water bodies near unconventional oil and gas (UOG) sites. While some biocides and their degradation products have been identified as chemicals of concern because of their toxicity, the selective antimicrobial pressure they exert has not received adequate attention. Overall, the use of biocides in various applications poses significant risks to the environment and human health. It is essential to carefully consider the potential risks and benefits of using biocides and to develop strategies to minimize their environmental impact.

These are only a few examples of harmful chemicals found in drilling cuttings. The specific chemicals in any given sample of drilling cuttings will depend on the type of drilling fluid used, geological formation being drilled, and other factors. It is important to properly manage drilling cuttings to prevent these chemicals from entering the environment and causing harm to human health. Incorrect disposal can harm human health and ecosystems, particularly through contamination of groundwater. Oil and gas drilling activities can lead to soil, water, and air pollution, posing health risks due to exposure to potentially hazardous drilling muds. To minimize harm, companies must prevent spills and effectively manage drilling waste using closed-loop systems, treatment, and recycling. Drilling waste treatment methods include physical, chemical, and biological processes, with bioremediation gaining popularity for its eco-friendliness and cost-efficiency despite being slow and challenging to control. Other approaches include waste reduction, recycling, and safe disposal methods such as landfilling and deep well injection.

A critical knowledge gap exists in understanding wellbore collapse during oil and gas exploration, particularly its environmental consequences and waste management solutions. This study delves into this crucial area, focusing on the following:

- Identifying key triggers of wellbore collapse.
- Assess the volume of drilling cuttings generated.
- Developing environmentally friendly waste management techniques to minimize the ecological impact.

Traditional methods, such as unlined pits, pose significant risks to groundwater and soil quality because of potential leakage and contamination. This is particularly concerning in regions, such as Sudan, where inadequate waste management practices exacerbate environmental harm. To address this critical issue, our research aims to:

1. Gain a comprehensive understanding of wellbore collapse triggers and their environmental consequences.
2. Advances in sustainable waste management systems for drilling cuttings, minimize their ecological footprint.
3. Develop practical strategies for effective drilling and cutting management in Sudan that are specifically tailored to its unique context.

The methodology involves the following steps:

- The effects of drilling fluids on wellbore stability were investigated through simulations and modelling.
- Assessing the impact of drilling cuttings on groundwater and soil quality.

This research has significant potential for the following reasons:

- Improved understanding of wellbore collapse and its environmental implications.
- Development of sustainable drilling practices in Sudan's oil and gas sector.
- Protection of human health and the environment through effective waste management.

By creating a more efficient and environmentally responsible drilling and waste management system, this research will meaningfully contribute to a sustainable future for Sudan's oil and gas industry.

## Theoretical background and literature review

While successful oil and gas extraction is based on the optimal performance of drilling fluids, particularly in difficult environments, conventional fluids often fail. Exploring novel additives to address these limitations is exciting research. For example, nanosilica particles enhance the rheological properties of both oil-based and water-based muds even at high temperatures, whereas polypropylene beads improve cutting transport in all well types, facilitating hole cleaning. Modified apatite ore is a better acid-soluble weighting agent that enhances density control, rheology, sag stability, and formation protection compared with limestone. Untreated durian rind with retained pectin is a sustainable alternative that effectively controls fluid loss and improves the rheology of water-based mud. These discoveries have opened the way for more efficient and environmentally friendly drilling. The fight does not end there. Shale formations, which are prone to instability due to drilling fluid infiltration, pose a different problem. Reservoir damage, another industry obstacle, reduces productivity and output. Although studies have dissected damage mechanisms and identified their sources, the adaptation of mitigation strategies to single wells remains largely unexplored. Drilling and workover fluids are often blamed for contributing to damage through solid and filtrate invasion, fluid-rock interactions, water blockage, salinity shock, and high sulfate content. To effectively combat this problem, it is necessary to integrate diverse datasets to provide valuable insights into the causes of damage and guide remediation strategies. Key measures include minimizing fluid invasion, carefully selecting fluid types and solids for stimulation treatments, conducting compatibility testing, and avoiding long-term fluid presence in boreholes. Pore throat plugging due to solid invasion and rock–fluid incompatibilities are the primary causes of formation damage induced by drilling and completion fluids. By emphasizing integrated data analysis, especially in low-permeability reservoirs and deepwater environments, the industry can design solutions to prevent damage and achieve optimal well performance [20–22].

Hany Gamal et al. (2022) [23]; used various techniques, including X-ray diffraction, scanning electron microscopy, nuclear magnetic resonance, and scratch testing, to assess changes in rock aeromechanics caused by exposure to mud filtrate. The study revealed decreased shear wave velocities owing to mineralogical modifications, which affect rock geotechnical characteristics that are crucial for petroleum industry applications. Fine migration during drilling and completion is a major contributor to formation damage in unconsolidated sandstone reservoirs. Nanoparticles have demonstrated effectiveness in controlling fine migration by adsorbing and fixing them, thus preventing pore throat blockage. Al2O3 nanoparticles exhibited the utmost performance, and nanoparticle suspensions with higher ionic strengths were preferred. A mathematical model was developed to calculate the interaction energy between the formation fines and the rock pore surface with adsorbed nanoparticles. This model provides insight into the microscopic mechanisms of fine migration control by nanoparticles. The results indicated that the nanoparticles formed an adsorption layer on the pore surface, enhancing their physical and chemical heterogeneities and promoting fine adsorption and fixation. This drives to a downward shift in the interaction energy curves of the fine and pore surfaces, reducing or eliminating repulsive barriers and increasing the attractive potential energy. These changes promote fine adsorption and fixation at the pore surface, effectively preventing damage to the formation.

Zhang et al. [24] in their 2021 study, explored wellbore instability within layered formations. Their investigation revealed that the manner in which collapses occur is influenced by the angle at which the bedding layer dip. Specifically, they noted that lower angles resulted in distinct collapses in specific directions, whereas higher angles directed to a more pronounced expansion of the wellbore diameter. Gaining insight into these collapse patterns is crucial for improving drilling safety. Shale formations are particularly susceptible to harm caused by oil-based drilling fluids, which can weaken the rock and ultimately result in wellbore collapse. To investigate this matter, Zhang et al. and their team [24], employed the downhole core method in their research. Their findings revealed a reduction in the compressive strength and cohesion of shale following exposure to drilling fluid, particularly when the bedding planes had steep angles. Furthermore, the study underscored a significant increase in collapse pressure, highlighting the critical importance of considering shale bedding angles in wellbore stability assessments.

Real-Time Optimization of drilling Parameters (RTOP) is a transformative technology that continuously monitors and adjusts drilling parameters to achieve optimal drilling performance. This cutting-edge approach has gained significant traction in the oil and gas industry because of its ability to enhance efficiency, reduce costs, and improve safety.

Accurately identifying the collapse pressure of a geological formation is of paramount importance in the intricate process of selecting the most appropriate drilling-fluid density. This critical factor plays a pivotal role in minimizing formation damage, which is a central focus in the quest to optimize productivity, particularly within the unique geological context of sandstone reservoirs interwoven with clay. Roof's pioneering work in 2018 introduced a groundbreaking methodology for analyzing wellbore stability in the context of drilling operations within the Presalt Formation, as exemplified by a case study conducted in southern Iran. This research serves as a valuable reference for understanding the complexities of drilling in difficult geological environments. Halim and his esteemed colleagues embarked on an exhaustive and comprehensive study in 2022, delving deep into the intricacies of minimizing formation damage during drilling operations within these sandstone-clay intercalated reservoirs. Their findings not only underscore the critical role played by this aspect in enhancing overall productivity but also offer practical insights for mitigating formation-related challenges. Furthermore, in 2020, Houbin and associates introduced a groundbreaking mathematical approach known as the "Continuous Tangent Envelope Method". This innovative methodology not only refines the precision of calculating the formation collapse pressure but also provides a more sophisticated and precise means of articulating this essential parameter, especially when dealing with the formidable complexities of tight sandstone formations. This advancement in methodology significantly bolsters the capacity to accurately assess and effectively manage the formation collapse pressure, thereby enhancing the reliability and precision of drilling operations [25–27].

The RTOP implementation offers numerous benefits, including reduced drilling costs and enhanced wellbore integrity. Despite its substantial benefits, RTOP faces challenges in terms of data quality, model development, and integration with drilling automation. However, advancements in data analytics, machine learning, and artificial intelligence are expected to further enhance RTOP's capabilities and effectiveness in the future. As drilling environments become increasingly complex and challenging, RTOP is poised to become an indispensable tool for optimizing drilling performance, reducing drilling costs, and ensuring wellbore integrity [28–33]. One of the most important parameters to consider is that efficient hole cleaning is critical for successful drilling operations. Researchers have explored the incorporation of additives into water- or oil-based mud to improve cutting transport. Horizontal wells with a slim hole (HW-SH) offer several advantages; however, the narrow annulus can become blocked, directing to increased annulus pressure. A new model was developed that accurately predicts the cutting transport law in the annulus of HW-SH drilling. In addition, a stability criterion was developed for the transition from laminar to turbulent flow of yield power law (YPL) fluids in concentric and eccentric annuli [34–40]. The combination of drilling evaluation and fines migration control presents promising solutions for preventing wellbore instability and formation damage in mature reservoirs and unconsolidated sandstone formations. These techniques, along with geomechanical modelling and integrated well planning, provide effective strategies for addressing drilling challenges in mature oil and gas fields. Together, these approaches can optimize drilling operations, minimize downtime, reduce costs, and provide effective waste management.

Drilling in depleted oil and gas fields is challenging, particularly in complex pore pressure regimes with overpressure zones. Traditional wellbore stability approaches rely on conservative mud density curves, which may not effectively address all drilling hazards [2, 41–43]. Radwan (2022) [44], introduced a dynamic approach called the "Depth of Damage (DOD)" to assess wellbore stability. This method considers changing the pore pressure and rock strength and offers a more precise evaluation to prevent wellbore failure. As conventional drilling methods are no longer adequate for mature reservoirs with complex pore pressure regimes, underbalanced drilling (UBD) was introduced as a crucial technique for such reservoirs; however, it carries an increased risk of borehole instability. Previous wellbore stability studies could not effectively prevent borehole instability issues because of their conservative mud-weight window determination. Successfully demonstrated the application of UBD in the Gulf of Suez Rift Basin for the first time by employing depth-of-damage analysis to guide mud weight selection. This approach has proven effective in preventing borehole instability and enhancing production performance. The combination of the depth-of-damage approach for UBD and the use of nanoparticles to control fine migration offers promising solutions for preventing wellbore instability and formation damage in mature reservoirs and unconsolidated sandstone formations.

Treacherous terrains, such as depleted fields and deepwater abyssal depths hold the oil and gas industry to the ever-present threats of wellbore instability and formation damage. But fear not, intrepid explorers! This study unveils a beacon of hope in the form of cutting-edge drilling and completion technologies, offering the industry a shield against these formidable foes. These innovations promise not only to bolster wellbore integrity, but also to pave the way for a more secure and efficient future, unlocking new reserves and ensuring a sustainable future for this vital sector.

## Methodology

This study will investigate the causes of wellbore collapse, assess the volume of drilling cuttings generated, and develop environmentally friendly waste management techniques. this will involve a thorough literature review and conceptual framework development, field data collection, computer modelling, environmental impact assessment, and waste management strategy development. This research is anticipated to enhance wellbore stability, reduce costs, and safeguard the environment. The investigation started with a comprehensive survey and data collection endeavour, drawing upon information gathered from the Al-Rateena-1 well, Block 25D, Al-Rawat field in Sudan. This strategically positioned locale lies near the city of Kosti within the White Nile State of Sudan. Renowned for its agricultural and pastoral significance, the region also harbors immense geological and petroleum potential.

The Al-Rteena-1 well was drilled as a wildcat well in the Rawat field, Block 25D, by the Rawat Petroleum Operating Company (RPOC). The well was spudded on November 18, 2017, with total planned total depth (TD) of 4400.00 m below the drilling floor (mDF). The actual TD of 3839.00 mDF was reached on March 17, 2018. The National Upstream Solution (NUS) provided comprehensive mud logging services for the drilling operation.

The mud logging unit, G1711, is a computerized system equipped that receives signals from external surface sensors. These signals are used to evaluate formation conditions, detect the presence of hydrocarbons, and monitor real-time drilling engineering parameters. The unit is equipped with the Data Drill Computer System, DIAMOCO's latest and most advanced well computer system, comprising two subsystems: the data acquisition system (i.e., front-end) and the data storage system (i.e., back-end).

During drilling of the Al-Rteena-1 well, remote monitors were installed on the rig floor, the company man's office, and the geological supervisor's office. Every morning, a daily geological report (DGR) summarizing the drilled formation and drilling parameters over the report interval was submitted to the geologist of the RPOC well site, accompanied by a copy of the master log if required. Every midnight, a daily drilling report (DDR) covering the drilling parameters and operations was submitted to the company man's office. The primary target of the Al-Rteena-1 well was to test and evaluate the oil potential in the Galhak reservoir. Galhak sand, Entra-Melute, Melute, and lower Yabus were identified as secondary targets. Sidewall Cores, Formation Multi Testers (FMTs), Conventional Core Descriptions, and Sidewall Core Descriptions were not required. Gas was recorded in some well intervals, and hydrocarbon shows were observed during drilling.

The optimal positioning of the Al-Rteena-1 well was meticulously determined by comprehensive analysis of geological data, 3D seismic interpretation, mud logging, operational considerations, geological reservoir data, previous seismic inversion results, and formation evaluation. This integrated approach resulted in the well profile and formation lithology illustrated in Fig. 1.

Mud waste is a significant byproduct of drilling operations and contains various contaminants, including drilling fluids, cuttings, and formation fluids. Mud waste can contaminate groundwater and surface water, posing a risk to wildlife. Mud waste control methods include treatment, disposal, and reuse. Treatment involves the removal of contaminants using physical, chemical, or biological processes. Disposal involves placing the mud waste in a landfill or designated disposal site. Reuse involves recycling mud waste for use in other drilling operations. Wellbore integrity, formation preservation, and mud waste control are critical aspects of drilling operations. By understanding the current challenges and existing solutions in the field, drilling operations optimization, downtime minimization, cost reduction, and effective waste management will be observed.

## Wellbore instability methods

To thoroughly investigate wellbore stability, precise depth determination is essential. To achieve this, a technique for determining True Vertical Depth (TVD) has been developed using a specialized tool that converts measured depth data into TVD. This tool uses an index reference dataset, meticulously constructed by compiling the deepest to shallowest values from all measured depth curves across various datasets. This refined depth determination technique facilitates a comprehensive understanding of the depth profile of the wellbore and enables the identification of potential instability zones. The tool's reliance on an extensive index reference dataset ensures its accuracy and applicability across a wide range of wellbore configurations. This conversion process enables a more accurate representation of the wellbore's vertical depth. To facilitate the indexing process, a reference dataset is constructed. This dataset is generated by arranging values from measured depth curves obtained from all relevant datasets. The arrangement is

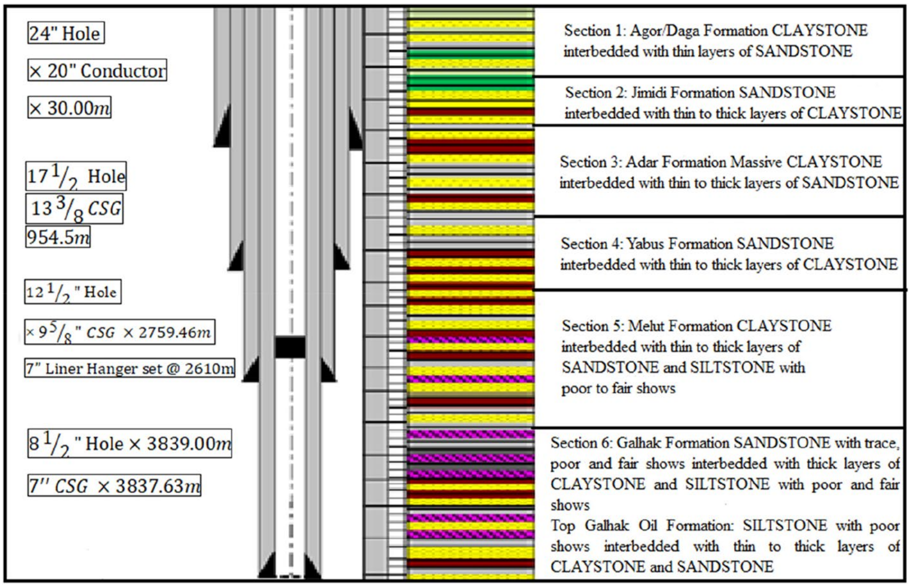

**Fig. 1** Well Al-Rteena-1 Profile, Structure Sketch, and Generalized Lithology Column. Wellbore integrity, formation preservation, and mud waste control are crucial aspects of drilling operations. Maintaining wellbore stability prevents the uncontrolled release of fluids or gasses, which can lead to lost circulation, stuck pipes, blowouts, and environmental damage. Several factors can contribute to wellbore instability, including the type of formation, drilling fluid, and drilling practices. Shale formations are particularly susceptible to collapse because of their bedding planes, and oil-based drilling fluids can weaken shale formations. Drilling in depleted oil and gas fields is further complicated by complex pore pressure regimes and overpressure zones. Traditional wellbore stability approaches, such as conservative mud density curves, are often inadequate in these challenging environments. Another major challenge in drilling operations occurs when drilling fluids and formation fluids interact, causing a reduction in permeability and porosity, leading to a significant decline in well productivity. Various mechanisms contribute to formation damage, including solid invasion, filtrate invasion, fluid-rock interactions, water blockage, salinity shock, and the high sulfate content of invading fluids. By integrating diverse datasets, the causes of formation damage can be identified, and effective remediation strategies can be developed

performed in descending order, starting from the deepest depth to the shallowest. This reference dataset serves as a crucial component in subsequent calculations.

Upon determining the depth, an estimation of the volume of shale ($\mathrm{V_{SH}}$) can be derived. This estimation, which is a crucial component of the methodology, is primarily based on gamma-ray measurements. The formula used for this estimation is given by Eq. (1).

$$\mathrm{V_{SH}} = \mathrm{GR_{index}} = \frac{GR - GR_{matrix}}{GR_{shale} - GR_{matrix}} \tag{1}$$

The density log records the bulk density of the formation, which is the cumulative density encompassing the solid matrix, formation fluid, and borehole fluid. Then, the total porosity is determined by subtracting the bulk density from the density of the solid matrix. The formula for calculating the total porosity (ØT) is expressed as Eq. (2).

$$Total\ Porosity\ Equation : \varnothing T = \frac{\rho_{ma} - \rho_B}{\rho_{ma} - \rho_f} \tag{2}$$

Additionally, the methodology addresses the estimation of total shale porosity ($ØT_{sh}$). This is accomplished by considering the density of the solid matrix, the bulk density, and the density of the shale component within the formation. The formula for calculating the total shale porosity is as follows (Eq. (3)):-

$$Total\ Shale\ Porosity(\varnothing T_{sh}) = \frac{\rho_{ma} - \rho_{sh}}{\rho_{ma} - \rho_{f}} \tag{3}$$

ascertain the effective porosity (ØE), the methodology subtracts the product of total shale porosity and the volume of shale from the total porosity. This step enables the calculation of the porosity that is relevant to reservoir evaluations, accounting for the presence of shale within the formation (Eq. (4)).

$$Total\ Effective\ Porosity(\varnothing E) = \varnothing T - (\varnothing T_{sh} \times V_{sh}) \tag{4}$$

This methodology uses the compound density log method as a relatively simple yet accurate approach to estimate the total porosity. It is important to consider the potential impact of borehole fluids and the distribution of fluids within the formation on the accuracy of this method. The methodology involves estimating the overburden stress by first calculating the average bulk density beneath the seafloor. This calculation was performed using an empirical equation based on statistical data related to the average bulk density. The equation is expressed as Eq. (5) as follows:

$$\rho_{AMOCO} + A_0 \times \left[\frac{(TVD - Air\ Gap - Water\ Depth)}{312}\right]^{\propto=0.6} \tag{5}$$

Equation (5) was developed by Amoco's Exploration and Production Research Group in the early 1980s, and is known as the AMOCO equation, an abbreviation for "Atlantic Richfield MObil COrporation". This equation assumes a linear increase in bulk density with depth, which is generally valid for shallow sediments but may not be accurate for deeper sediments that have undergone compaction or diagenesis. While relatively simple and effective, the AMOCO equation has limitations. The assumption of a linear increase in bulk density may not always hold, especially for deeper sediments. Additionally, the equation does not account for the presence of gas or oil within the sediment layer, which can affect the bulk density. Finally, the equation relies on accurate measurements of the travel time and thickness of sediment layers, which can be challenging to obtain. Despite these limitations, the AMOCO equation remains a commonly used method in seismic surveys for hydrocarbon exploration and geotechnical engineering projects.

The overburden stress is defined as the pressure exerted by the weight of the rock formations located above the point of interest. It accounts for the cumulative mass of the overlying rock and sediments and is a critical parameter in geomechanical assessments.

The Eaton method to predict pore pressure within a geological formation was employed as a predictive approach that relies on specific formation properties, including sonic velocity and density. Sonic velocity is a fundamental parameter used in this methodology. It represents the speed at which sound waves propagate through the geological formation. Sonic velocity measurements provide crucial insights into the physical characteristics of the formation. The methodology also considers the density of the formation. Density represents the mass of material within a unit volume of the formation and is another essential property used for pore pressure prediction. Then prediction of pore pressure ($\mathrm{P_P}$) is achieved through the application of the Eaton method, which utilizes the following Eq. (6):

$$P_P = (\sigma_v - PP_{norm}) \times \alpha \times \left(\frac{R}{R_{norm}}\right)^n \tag{6}$$

The Eaton method can be used to predict pore pressure from measurements of sonic velocity or resistivity. The equations for the Eaton method are as follows:

In linear trendlines:

$$\mathrm{P} = \mathrm{aZ^\wedge n} + \mathrm{P_{norm}} \tag{7}$$

In semi-log trendlines:

$$\log(\mathrm{P}) = \mathrm{aZ^\wedge n} + \log(\mathrm{P_{norm}}) \tag{8}$$

This harnesses the power of the Eaton method, which integrates measurements of sonic velocity and formation density to project pore pressure within the geological strata. The predictive equation, tailored to consider the unique attributes of the formation, offers invaluable insights into the subsurface conditions. These insights hold substantial utility across a spectrum of applications within the oil and gas industry. It is crucial to acknowledge that the accuracy of the Eaton method can be influenced by factors such as the presence and distribution of borehole fluids. In addition, the careful selection of appropriate values for the Eaton factor and exponent plays a pivotal role in the precision of the predictions.

The estimation of the fracture gradient (FG) is accomplished using Eq. (9):

$$FG = K * (\sigma v - p) + \alpha Pp \tag{9}$$

Notably, various fracture gradient estimation methods differ primarily in how they compute the stress ratio (K). The specific methodology chosen can affect the accuracy of the fracture gradient prediction. Two common methods are highlighted:

- Eaton Method: This method involves inputting the effective Poisson ratio through a curve or using constant values segmented by zones, followed by the computation of K.
- Eaton—Gulf Coast Method: This variant calculates the effective Poisson's ratio using empirical correlations derived from data specific to the Gulf coast region and subsequently computes K.

The determination of the elastic shear slowness properties relies on the analysis of the isotropic properties, which encompass the bulk density, compressive slowness, and shear slowness. These properties play a pivotal role in the characterization of subsurface formations.

The dynamic bulk modulus ($\mathrm{K_{dyn}}$) is computed using Eq. (10) as follows:

$$\text{Dynamic Bulk Module}(\mathrm{K_{dyn}}) = \left\{\frac{(13474.45)\rho_b}{\left(\Delta \mathrm{t_{comp}}\right)^2}\right\} - \frac{3}{4} \tag{10}$$

The dynamic shear modulus ($\mathrm{G_{dyn}}$) is determined using Eq. (11):

$$\text{Dynamic Shear Modulus}(\mathrm{G_{dyn}}) = \left\{\frac{(13474.45)\rho_b}{(\Delta \mathrm{t_{Shear}})^2}\right\} \tag{11}$$

The dynamic Young's modulus ($\mathrm{E_{dyn}}$) is computed using Eq. (12):

$$\text{Dynamic Young}'\text{s Modulus } \mathrm{E_{dyn}} = \frac{9\mathrm{G_{dyn}} \times \mathrm{K_{dyn}}}{\mathrm{G_{dyn}} + 3\mathrm{K_{dyn}}} \tag{12}$$

The dynamic Poisson ratio ($\mathrm{V_{dyn}}$) is determined using Eq. (13):

$$\text{Dynamic Poission Ratio} = \mathrm{V_{dyn}} = \frac{3\mathrm{K_{dyn}} - 2\mathrm{G_{dyn}}}{6\mathrm{K_{dyn}} + 2\mathrm{G_{dyn}}} = \frac{R_{sp}^2 - 2}{2R_{sp}^2 - 2} = \frac{\left(\Delta t_{shear}^2/\Delta t_{comp}^2\right) - 2}{2\left(\Delta t_{shear}^2/\Delta t_{comp}^2\right) - 2} \tag{13}$$

The static Poisson Ratio ($\mathrm{PR_s}$) is derived by multiplying the dynamic Poisson ratio ($\mathrm{PR_d}$) by a dimensionless PR multiplier. When the PR multiplier is set to its default value of 1.0, $\mathrm{PR_s}$ equals $\mathrm{PR_d}$. This transformation allows for the consideration of static properties alongside dynamic measurements.

The static bulk modulus ($\mathrm{K_{sta}}$) and static shear modulus ($\mathrm{G_{sta}}$) were calculated using theoretical equations based on experimental measurements. These calculations are performed as follows (Eq. (14)):

$$G_{sta} = \frac{E_{sta}}{2(1 + v_{sta})} \text{ and } K_{sta} = \frac{E_{sta}}{3(1 - 2v_{sta})} \tag{14}$$

The Coates Denoo Correlation was employed to estimate the unconfined compressive strength (UCS) in rock strength analysis. The correlation is expressed by Eq. (15).

$$C_0 = 0.0866 \times \left[\frac{E_{dyn}}{C_{dyn}}\{0.008V_{sh} + 0.0045(1 - V_{sh})\}\right] \text{ where } C_{dyn} = \frac{1}{K_{dyn}} \tag{15}$$

A linear correlation was used to map the Gamma Ray (GR) to the friction angle (FANG) then, tensile strength ($\mathrm{T_{STR}}$) is directly calculated from the UCS strength using a factor (K). The formula is as follows (Eq. (16)):

$$\mathrm{COH} = \frac{\mathrm{UCS}}{2\left\{\sqrt{1 + (\tan \mathrm{FANG})^2} + \tan \mathrm{FANG}\right\}} \text{ where } \mathrm{T_{STR}} = \mathrm{K} \times \mathrm{UCS} \tag{16}$$

Where: K is a factor that can vary on the basis of facies and zone characteristics with a default value of 0.1. This default value aligns with the Griffith elastic-brittle theory, which establishes a compressive strength to tensile strength ratio in the range of 8 to 12.

Well log data are a fundamental component of this methodology for predicting subsurface pore pressure. These data, gathered from various tools, provide insights into geological formations, including rock density, porosity, and fluid content. Integrating well log data with other geophysical and geological information enhances the accuracy of pore pressure models, ensuring wellbore stability, reducing drilling risks, and optimizing hydrocarbon recovery (Fig. 2).

This methodology combines various analytical approaches and models to predict pore pressure, assess rock strength, and use well log data for efficient drilling and improved hydrocarbon recovery. It encompasses the integration of static and dynamic properties, providing valuable insights for the development of subsurface exploration and drilling operation.

## TechLog software

TechLog is a software platform owned by Schlumberger and, specifically designed to operate on the Windows operating system. It serves as a comprehensive toolset with the primary objective of consolidating all wellbore data types, providing users with the capability to analyze a diverse range of log and core data. TechLog is adept at

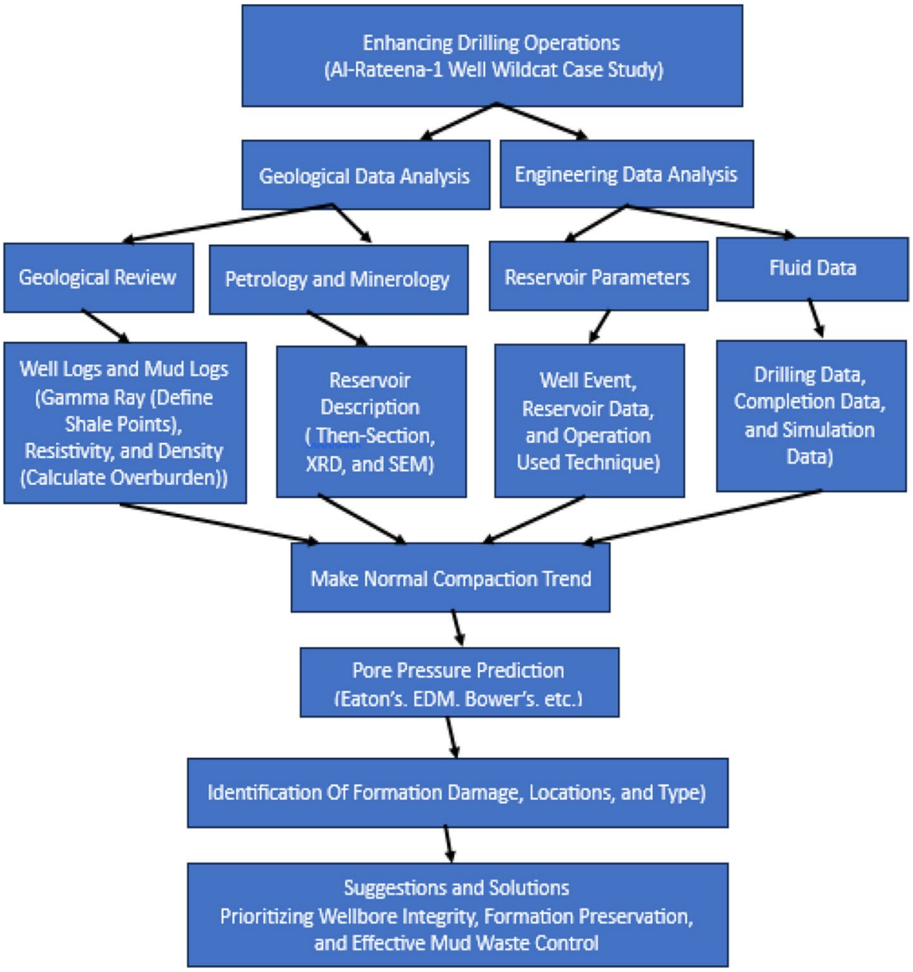

**Fig. 2** Leveraging well log data for improved pore pressure prediction

fulfilling a crucial requirement in the field of wellbore data management and analysis. Its core functionality revolves around the consolidation of wellbore data, offering users a unified platform to handle various data types. This includes logs, core data, and other pertinent information related to wellbore operations. The platform excels in bringing together a wide array of wellbore data, eliminating the need for users to employ multiple specialized tools for individual data types. This unification simplifies the data analysis process and enhances the overall efficiency of the wellbore data interpretation tasks. A distinct advantage of TechLog is its capacity to facilitate continuous risk and uncertainty evaluation throughout the lifecycle of a wellbore. By providing a centralized repository for all relevant data, it enables users to make informed decisions and assess potential risks at every stage of wellbore operation. The key benefits are:

- Streamlined Data Handling: TechLog's consolidation capabilities streamline the management of diverse wellbore data types.
- Enhanced Efficiency: Users benefit from increased efficiency in data analysis and interpretation, eliminating the need to switch between multiple tools.
- Informed Decision-Making: The platform supports well-informed decision-making by facilitating risk and uncertainty evaluation throughout the wellbore lifecycle.

The methodology revolves around TechLog, a platform that streamlines data management and interpretation by consolidating and analyse diverse wellbore data. It fosters informed decision-making and continuous risk assessment throughout the wellbore's lifespan. Following thorough preparations and evaluations based on data extracted from the well's internal reports, the researcher meticulously prepared the TechLog platform, incorporating necessary corrections. This refined platform serves as the foundation for real-time analyses and informed decision-making, maximizing its effectiveness.

## Waste management methods

Oil and gas extraction poses a significant environmental challenge because of persistent pollution issues. Drilling operations, in particular, are complex and generate various pollution sources. Among these, the pump-circulation system stands out as the primary culprit. This system, which is crucial for drilling activities, including well cleaning, relies on drilling mud with specific rheological properties. This drilling mud serves multiple purposes, including thorough hole cleaning and optimizing drill bit performance. The proposed methodology addresses this environmental challenge by focusing on drilling fluid management, specifically drilling mud. This study emphasizes the importance of effective drilling fluid management, particularly drilling mud, to streamline drilling processes, enhance hydraulic performance, and minimize the environmental impact of oil and gas extraction. In the issue of the environmental impact study, the methodology for analysis was to taking samples of mud, drill cuttings, and soil. This process includes:

1. Excavation and Observation: The chosen site is excavated to a maximum depth of 4 m using a mechanized excavator, or approximately 1.5 to 2 m if hand tools are

employed. The hole's width should allow for cross-section observation and delineation of geological or contaminant horizons. Cross-sectional photographs are recommended if feasible.

2. Sampling Strategy: In general, an integrated sample from the entire hole depth is collected. However, multi-level sampling may be considered on a case-by-case basis, especially if soil types or contamination levels vary significantly.
3. Soil Description: The soil/sediment is characterized based on the basis of grain-size, colour, texture, and odor, noting any variations between layers.
4. Location Recording: Sample locations are recorded using a handheld GPS and marked on appropriately scaled maps.
5. Sample Collection and Labelling: Approximately 100 g of soil is collected and placed in a plastic bag. Sample numbering follows the format S1.2, where S signifies soil (S for sediments, W for water, etc.), 1 represents the first site, and 2 indicates the second subsurface sample from site 1.
6. Analysis Parameters: A suite of analysis parameters is chosen on the basis of specific requirements (XRF Screening and Chemical Analysis).
7. Grain-Size Analysis: Grain-size distribution curves may be determined at certain sites, depending on the need.
8. Sample Storage: An unused portion of the sample is stored at the laboratory for up to one month in case additional analysis is required.
9. Cross-Contamination Prevention: Before sampling each new location, the sampling spoon is thoroughly cleaned to prevent cross-contamination.

## Results and discussions

By leveraging an array of well log data, including calliper measurements, bit size, gamma ray readings, bulk density, resistivity porosity, shale volume, and spontaneous potential, it was aimed to establish a meaningful correlation with intervals of wellbore instability, as depicted in Fig. 3. This figure provides a holistic assessment of wellbore conditions by combining critical well-log data, furnishing valuable insights both the stability and performance of the wellbore. Figure 3 further elucidates the fluctuations in wellbore conditions within various intervals, with a particular focus on areas prone to instability. The combination of well log data with these instability intervals enables the discernment of noteworthy trends, thereby significantly contributing to the enhancement of drilling and maintenance strategies. This analytical approach ultimately fortifies the integrity of the wellbore and enhances operational efficiency.

Figure 4 visualizes the depict profound relationship between shear slowness in a relation to the estimated Poisson ratio and depth, a crucial factor in comprehending the fundamental properties and behaviours of subsurface formations. The analysis of the data and trends presented in this figure yields valuable insights into the utility of shear slowness as an indicator of deformation behaviour. These insights hold immense significance in obtaining a comprehensive grasp of subsurface characteristics, which, in turn, serve as the cornerstone for informed decision-making and predictions, and the foundation for more precise modelling and analysis of geological materials and formations.

This study underscores the pivotal role of isotropic properties, encompassing static Poisson's ratio, static Young's modulus, bulk modulus coefficient, and friction angle,

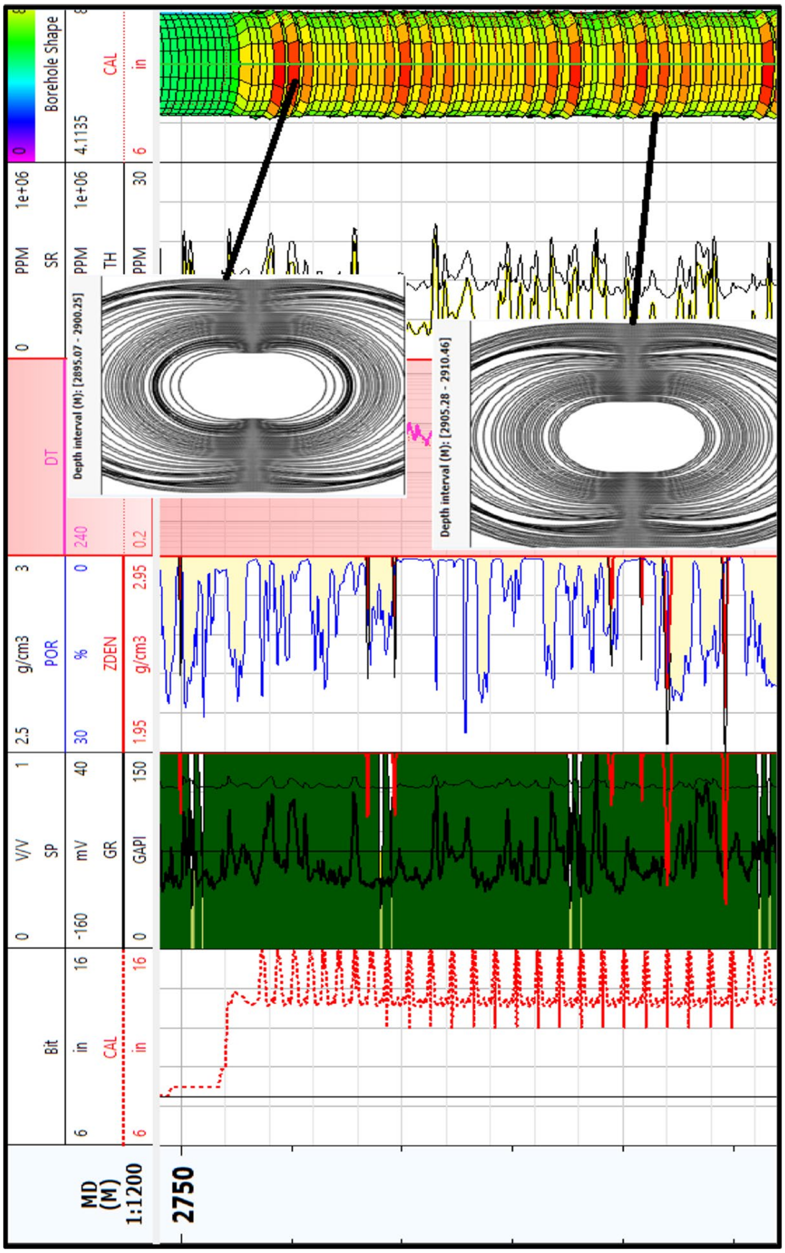

**Fig. 3** Visualizing the wellbore condition through the interval instability plot of log data

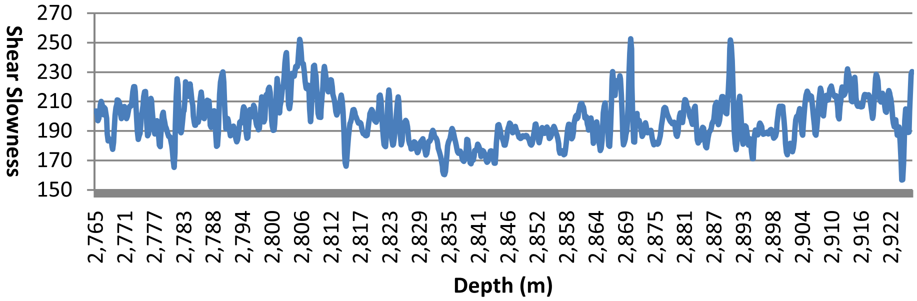

**Fig. 4** Shear slowness

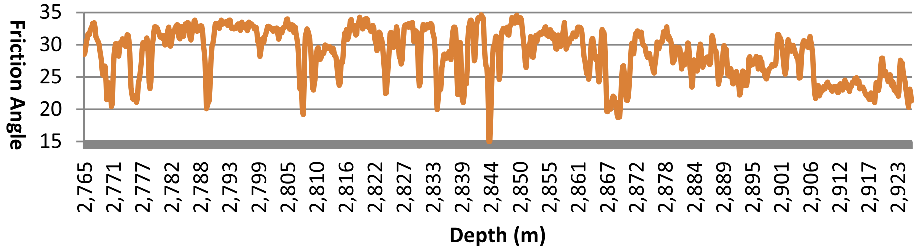

**Fig. 5** Friction angle

in elucidating material behaviour. These properties offer essential insights into various aspects of material response, including its reaction to stress-induced contractions or expansions (static Poisson's ratio), its stiffness (static Young's modulus), and its responsiveness to pressure changes (bulk modulus coefficient). Additionally, the friction angle provides critical information about a material's resistance to sliding and shear failure, adding to the understanding of geological formations under investigation.

One significant outcome of this study is the establishment of a linear correlation between Gamma Ray (GR) values and the Friction Angle (FANG), a pivotal parameter in geotechnical analysis. The default parameters set GR values of 120 gAPI to correspond to FANG values of 20 degrees and GR values of 40 gAPI to align with FANG values of 35 degrees. However, to cater to specific geological conditions, the methodology allows for flexible adjustment of these parameters. Figure 5 visually depicts this correlation and highlights its sensitivity to changes in these parameters.

To ensure stability and consistency in the analysis, a minimum FANG of 15 degrees was imposed when the calculated values fell below this threshold. Conversely, FANG values exceeding 40 degrees were capped at 40 degrees for practicality and analytical consistency. This parameter customization feature empowers precise mapping of Gamma Rays to the Friction Angle, accommodating the unique geological intricacies and project requirements encountered. This adaptability and precision underscore the methodology's robustness and capacity to yield accurate, contextually relevant insights.

A crucial poro-elastic parameter was computed, serving as a key determinant of the compressibility inherent to the dry skeletal framework within the rock matrix. This parameter assumes a pivotal role in understanding rock formations by shedding light on the compressibility characteristics of the dry skeletal structure of the rock matrix's. Figure 6 provides a visual representation of this calculated poro-elastic parameter,

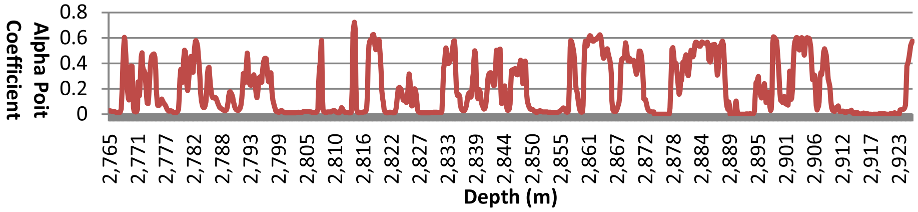

**Fig. 6** Alpha boit coefficient

facilitating a graphical assessment of its fluctuations across diverse conditions or positions within the rock matrix. This visual depiction significantly augments the capacity to comprehend the spatial distribution and significance of this parameter, thereby contributing to a deeper insight into the behaviour of rock formations.

This specific elastic constant assumes a pivotal role as a fundamental gauge of a material's compressibility when it encounters stress in a direction perpendicular to the applied force. Essentially, it quantifies the relationship between a material's lateral strain and its longitudinal strain, providing a precise ratio that characterizes its response to external stressors. Figure 7 assumes the role of a graphical representation, depicting the computed values of this elastic constant and furnishing a lucid visual representation of its fluctuations across various conditions or scenarios. This graphical presentation significantly enhances the ability to discern how this elastic constant varies in response to different circumstances, thereby deepening the understanding of the material's behaviour.

Young's modulus is fundamental parameter that serves as a pivotal elastic constant that precisely quantifies the interplay between longitudinal stress and longitudinal strain within a material. This numerical characterization of Young's modulus has been diligently calculated and is thoughtfully depicted in Fig. 8.

Accurate estimation of pore pressure (PP) and fracture gradients (FG) within a wellbore is of paramount importance in establishing a safe mud weight range for drilling operations, thereby mitigating the risk of wellbore instability. Several methodologies

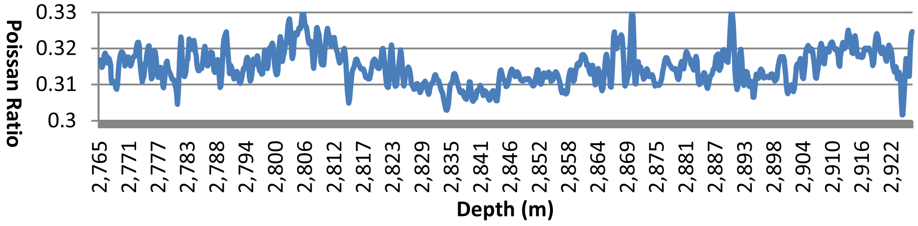

**Fig. 7** Poisson ratio

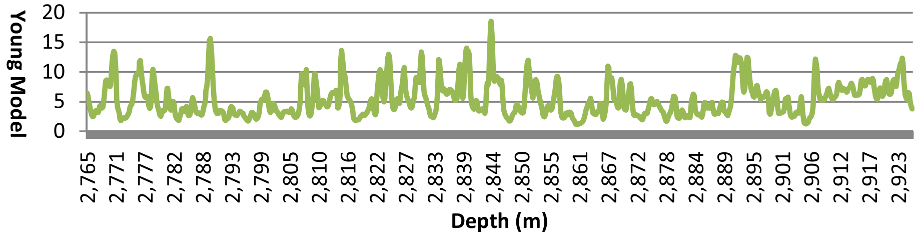

**Fig. 8** Young model

leverage the principles of vertical-effective stress, rooted in Terzaghi's law, to estimate pore pressure. These approaches account for stress-induced phenomena such as compaction and changes in elastic wave velocity through the concept of effective stress. Overburden stress is determined using bulk density data to assess the weight per unit area of the rock column above a specific point within the wellbore. Meanwhile, the calculation of effective vertical stress often necessitates the use of logging measurements or seismic data, especially when dealing with shale formations. For permeable zones, pore pressure estimation typically involves linear interpolation between adjacent shale data points. These collective methods and calculations play a pivotal role in ensuring the safety and efficiency of drilling operations, while simultaneously minimizing the risks associated with pressure differentials and rock fracturing, as illustrated in Fig. 9.

It is crucial to recognize that the driller exerts direct control over radial stress by making choices related to mud density and drilling techniques. In contrast, axial and tangential stresses within the wellbore are consequences of the wellbore pressure, which is a factor within the driller's command. To foster a deeper comprehension of these relationships, it is advantageous to visualize wellbore stresses concerning the Equivalent Circulating Density (ECD), a parameter directly adjustable by the driller.

The ECD represents the measured annular pressure downhole, which is transformed into a mud density value to simplify interpretation for the driller. It encompasses the static mud density alongside additional pressures stemming from mud pumps and drill string motion. Figure 10 is typically employed to illustrate these dynamics in the form of a wellbore stress diagram. This diagram depicts a vertical well with uniform horizontal stresses and visually portrays the interplay of wellbore stresses concerning variations in ECD. Specifically, it elucidates that radial stress escalates with increasing ECD, whereas tangential stress diminishes with rising ECD. Remarkably, axial stress remains unaffected by ECD fluctuations. Across most ECD ranges, wellbore stresses predominantly exhibit a compressive nature. However, at extremely low ECD values, the radial stress transitions to a tensile state, and conversely, at exceedingly high ECD values, the tangential stress becomes tensile.

Understanding these wellbore stress behaviours is instrumental in defining the safe mud weight window for drilling operations. This safe window, as delineated by the data and relationships presented in Fig. 9, serves as a critical reference point for drillers, ensuring the maintenance of wellbore stability and safety throughout drilling operations.

Figures 10 and 11 provide a comprehensive examination of wellbore stability in relation to the depth of damage, yielding insightful results and discussions:

1. Red Curve (CMW_MIN_MC—Initial Breakout Limit): This curve represents the initial wellbore shear failure gradient, often referred to as "breakout." When the mud weight falls below this critical breakout threshold, shear failure within the borehole becomes imminent, resulting in a 0% depth of damage scenario.
2. Yellow Shade (5% Wellbore Damage): The yellow shaded region signifies the limit at which the extent of borehole failure is constrained to 5% or lower. Maintaining the mud weight within this range ensures manageable borehole damage, enabling effective borehole cleaning during drilling operations.

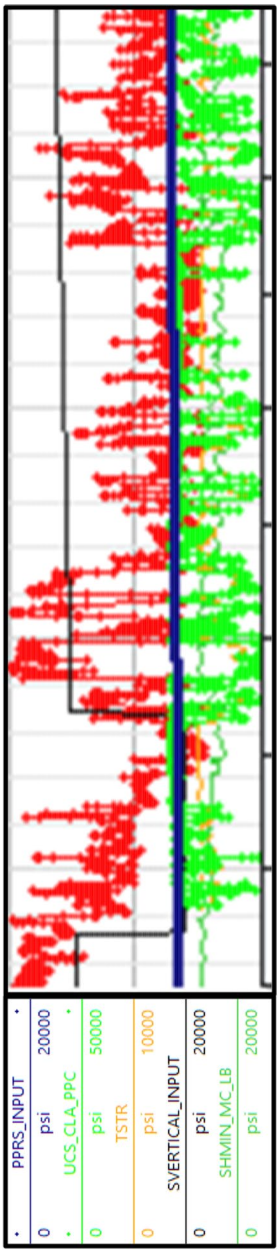

**Fig. 9** Geomechanical pressure

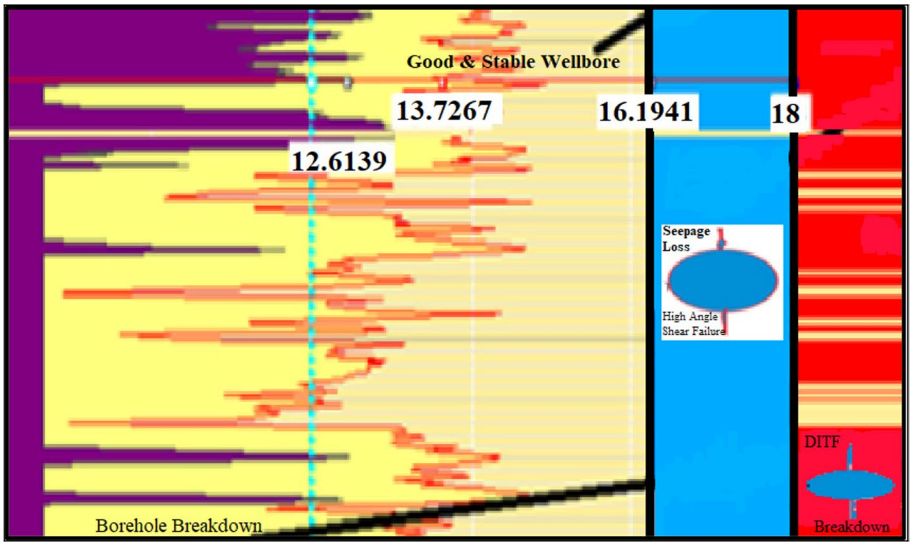

**Fig. 10** Visualizing wellbore failure modes in response to mud weight variations

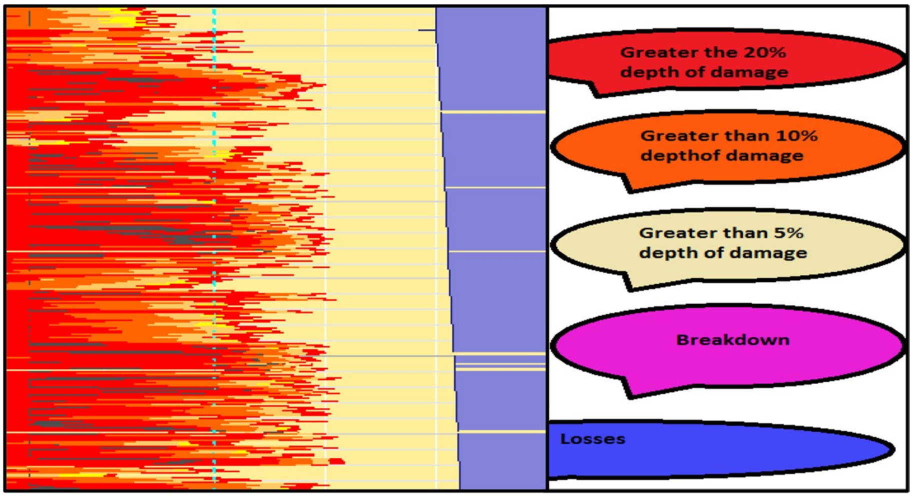

**Fig. 11** Assessing wellbore stability and damage depth

3. Orange Shade (10% Damage): The orange shaded area denotes the limit at which borehole damage reaches 10% or less when operating within this mud weight range.
4. Brown Shade (20% Damage): The brown shaded region signifies the limit where borehole failure remains limited to 20% or less, ensuring acceptable wellbore stability.

Analysis of the information presented in Fig. 10 highlights the inadequacy of drilling fluid with a density of 10 pounds per gallon (ppg) in achieving balance with the drilling formation. This deficiency results in formation collapse, as vividly illustrated in Fig. 11. These findings underscore the critical importance of effective mud weight management in ensuring wellbore stability during drilling operations.

The calculation process considered several key factors, including the cumulative cuttings volume, concentration levels, the use of water-based mud, the volume of mud designated as “mud waste” in the cuttings pit, and a thorough record of pit excavation, lining, and capping.

Using data extracted from drilling fluids reports, the values of $\theta_{600}$, $\theta_{300}$, N, and K were computed specifically the impacted zone of the well, ranging from 2775 to 2925 m. The detailed results of these calculations are comprehensively presented in Table 1. The calculation outcomes reveal a noticeable decrease in the value of K within the affected area, whereas the variation in N remains minimal and lacks significant implications.

Drilling fluid performance is significantly affected by contaminants. In the unaffected zone, the fluid exhibits superior performance, effectively transporting large cuttings without compromising its rheological properties or gel strength. This is attributed to higher PV and YP values. Conversely, in the affected zone, lower PV and YP values reflect compromised rheology and gel strength. However, these lower values maintain adequate fluid circulation and prevent excessive wellbore pressure buildup. In the affected zone, the fluid exhibits a higher mean N value equal to (0.540) and a smaller standard deviation (0.0062) compared with the unaffected zone. This indicates a higher density and a more uniform distribution of fluid particles in affected zone. These characteristics suggest that the contaminated fluid is more viscous and less fluidous than the clean fluid. This difference in fluid behaviour likely arises from impurities or contaminants causing fluid particles to clump together. In contrast, the unaffected zone exhibits a lower mean N value (0.555) and a smaller standard deviation (0.0027) compared with the affected zone. This indicates a lower density and a more uniform distribution of fluid particles in the unaffected zone. These characteristics suggest that the clean fluid is less viscous and more fluid than the contaminated fluid. This difference in fluid behaviour likely arises from the absence of impurities or contaminants in the clean zones. In summary, fluid behaviour in the affected zone differs significantly from that in the unaffected zone. The presence of impurities or contaminants leads to more viscous and less fluid behaviour in contaminated zone compared with the clean zone, where fluid particles are more dispersed and less resistant to flow. Calculations for both the affected and unaffected zones reveal a substantial increase in effective viscosity. This notable change in drilling fluid viscosity has implications for drilling operations in these regions. The shift in effective viscosity can influence various aspects of drilling, including fluid circulation, cuttings transport, and overall wellbore stability. To ensure the continued smooth and efficient progress of drilling operations in both contaminated and clean areas, a comprehensive analysis of the underlying reasons behind this viscosity alteration is crucial.

The calculation process involved determining the average velocity, denoted as $V'$, around the drill pipe and assessing the effective viscosity, represented as ($\mu e$). These calculations were based on data extracted from the drilling report, encompassing drilling parameters from both the impacted zone (2775-2925 m) and the unaffected zones (3434-3626 m), as outlined in Table 2. These computations play a pivotal role in evaluating fluid behaviour and performance across different sections of the wellbore.

The results of the calculations conducted for both the affected area and the unaffected zones reveal a marked increase in the effective viscosity. This noteworthy change in the drilling fluid’s viscosity has implications for drilling operations in these regions. Based

**Table 1** Calculation of drilling fluid rheological properties

| **PV** | | **YP** | | **$\theta_{600}$** | | **$\theta_{300}$** | | **N** | | **K** | | **MD** | |
|---|---|---|---|---|---|---|---|---|---|---|---|---|---|
| **Affected** | **Unaffected** | **Affected** | **Unaffected** | **Affected** | **Unaffected** | **Affected** | **Unaffected** | **Affected** | **Unaffected** | **Affected** | **Unaffected** | **Affected** | **Unaffected** |
| 21 | 27 | 26 | 31 | 68 | 85 | 47 | 58 | 0.53 | 0.551 | 1,69 | 1.87 | 2775 | 3434 |
| 22 | 27 | 25 | 31 | 69 | 85 | 47 | 58 | 0.55 | 0.551 | 1.48 | 1.87 | 2790 | 3477 |
| 22 | 27 | 25 | 30 | 69 | 84 | 47 | 57 | 0.55 | 0.559 | 1.48 | 1.75 | 2843 | 3477 |
| 21 | 23 | 25 | 30 | 67 | 76 | 46 | 53 | 0.54 | 0.52 | 1.57 | 2.07 | 2894 | 3487 |
| 22 | 23 | 25 | 30 | 69 | 76 | 47 | 53 | 0.55 | 0.52 | 1.48 | 2.07 | 2969 | 3562 |
| 22 | 23 | 25 | 32 | 69 | 78 | 47 | 55 | 0.55 | 0.504 | 1.48 | 2.37 | 3022 | 3626 |

**Table 2** Determining average velocity at affected interval

| Flow Rate (GPM) | | N | | K | | V′ | | μe (CP) | |
|---|---|---|---|---|---|---|---|---|---|
| Affected | Unaffected | Affected | Unaffected | Affected | Unaffected | Affected | Unaffected | Affected | Unaffected |
| 512 | 507 | 0.533 | 0.551 | 1,69 | 1.87 | 266 | 263 | 75.69 | 83.58 |
| 524 | 509 | 0.554 | 0.551 | 1.485 | 1.87 | 272 | 264 | 66.09 | 83.44 |
| 522 | 508 | 0.554 | 0.559 | 1.485 | 1.75 | 271 | 263.4 | 66.19 | 80.42 |
| 494 | 509 | 0.542 | 0.52 | 1.57 | 2.07 | 256 | 264 | 68.78 | 82.43 |
| 508 | 508 | 0.554 | 0.52 | 1.485 | 2.07 | 263 | 263.4 | 67.09 | 82.52 |
| 517 | 509 | 0.544 | 0.504 | 1.485 | 2.37 | 268 | 264 | 66.553 | 88.79 |

on the provided information, the flow around the Drill Pipes exhibits characteristics of both laminar and turbulent flow. The higher average velocity in the affected zone suggests turbulent flow, whereas the lower average velocity in the unaffected zone suggests laminar flow. This indicates that the flow regime transitions from laminar to turbulent as the velocity increases. The transition from laminar to turbulent flow is often triggered by the presence of disturbances, such as the Drill Pipes, which introduce irregularities into the flow. The shift in effective viscosity can influence various aspects of drilling, including fluid circulation, cuttings transport, and overall wellbore stability. To ensure the continued smooth and efficient progress of drilling operations in both the affected and unaffected areas, it is imperative to delve deeper into the underlying reasons behind this viscosity alteration and conduct a comprehensive analysis.

The slip velocity (Vs) was calculated from information regarding stratified sequences found in the logging data and drilling parameters, as detailed below:

- Claystone interval: 120 m with a density of 18.36 pounds per gallon (ppg).
- Sandstone interval: 10 m with a density of 21.28 ppg.
- Siltstone interval: 5 m with a density of 17 ppg.
- Total interval length: 135 m.
- Assume a claystone diameter of 0.32 inches in the damaged interval.
- Assumption of a diameter change of 0.9 inches in the damaged interval.

Specifically, within the interval spanning from 2765 to 2914 m, the geologic composition consists of claystone interbedded with minor sandstone and minor siltstone. Here are additional details about this geological interval:

- The drilling operations within this interval maintained an average rate of penetration (ROP) of 1.7 m per hour, with a maximum ROP of 11 m per hour and a minimum ROP of 0.31 m per hour.
- The claystone in this interval exhibits characteristics such as medium to dark grey, occasional dusky brown, and traces of moderately olive brown and greenish grey. It ranges from moderately hard to hard in texture, is occasionally very hard, and displays a trace of stickiness. The claystone is described as sub-blocky to blocky, with minor silty and occasional earthy qualities. Traces of sandy and occasionally shaly features are also noted, with a slight to moderate calcareous content.

- The sandstone present is described as transparent to translucent and generally unconsolidated. There are instances of minor to moderately consolidated sections. The grain size ranges from very fine to fine, with abundant fine-grained and common very fine-grained areas. The sandstone exhibits a rounded to well-rounded texture, with well-sorted quartz grains. It occasionally contains an argillaceous matrix and calcareous or kaolinitic cement. The porosity is poor, and there are no visible shows.
- The siltstone is medium-light grey, with minor light olive grey and traces of off-white. It varies from moderate to well-indurated, with minor areas that are firm and occasionally soft. The siltstone is sub-blocky, with occasional amorphous features and a transition to very fine sandstone. It predominantly consists of quartz and may contain an argillaceous matrix, occasional calcite, traces of kaolinitic cement, and occasional calcareous cement. Porosity is poor, and no-shows are observed.

This detailed geological context provides the foundation for the calculation of slip velocity (Vs), which is a critical parameter in drilling operations and the assessment of drilling fluid behaviour in this complex stratified interval. Based on the calculations presented above, it is evident that an increase in slip velocity was observed both in the affected area and in the unaffected zone. This signifies a notable alteration in slip velocity, indicating changing dynamics within these regions, Table 3.

The calculation of the transport or lift velocity, referred to as (Vt), is derived by subtracting the slip velocity of particles from the annular velocity of the mud, with a comprehensive breakdown presented in Table 4. Notably, the outcomes of these calculations indicate a reduction in transport velocity, evident both within the impacted area and the unaffected zone. This decline in transport velocity signifies altered conditions that affect the movement of particles in these regions.

**Table 3** Calculation of slip velocity in affected interval

| **Vs for Claystone** | | | **Vs for sandstone** | | | **Vs for siltstone** | | |
|---|---|---|---|---|---|---|---|---|
| **MW (PPG)** | **μe (CP)** | **Vs** | **MW (PPG)** | **μe (CP)** | **Vs** | **MW (PPG)** | **μe (CP)** | **Vs** |
| 10.0 | 75.69 | 71.27 | 10.0 | 75.69 | 87.04 | 10.0 | 75.69 | 63.31 |
| 10.0 | 66.09 | 74.57 | 10.0 | 66.09 | 91.06 | 10.0 | 66.09 | 66.24 |
| 10.0 | 66.19 | 74.53 | 10.0 | 66.19 | 91.01 | 10.0 | 66.19 | 66.2 |
| 10.0 | 68.78 | 73.58 | 10.0 | 68.78 | 89.85 | 10.0 | 68.78 | 65.36 |
| 9.9 | 67.09 | 75.04 | 9.9 | 67.09 | 91.44 | 9.9 | 67.09 | 66.76 |
| 10.0 | 66.553 | 74.39 | 10.0 | 66.553 | 90.85 | 10.0 | 66.553 | 66.08 |

**Table 4** Calculation of transport velocity in affected interval

| **Vt for Claystone** | | | **Vs for sandstone** | | | **Vs for siltstone** | | |
|---|---|---|---|---|---|---|---|---|
| **V′** | **Vs** | **Vt** | **V′** | **Vs** | **Vt** | **V′** | **Vs** | **Vt** |
| 266 | 71.27 | 194.73 | 266 | 87.04 | 178.96 | 266 | 63.31 | 202.69 |
| 272 | 74.57 | 197.43 | 272 | 91.06 | 180.94 | 272 | 66.24 | 205.76 |
| 271 | 74.53 | 196.47 | 271 | 91.01 | 179.99 | 271 | 66.2 | 204.8 |
| 256 | 73.58 | 182.42 | 256 | 89.85 | 166.15 | 256 | 65.36 | 190.64 |
| 263 | 75.04 | 187.96 | 263 | 91.44 | 171.56 | 263 | 66.76 | 196.24 |
| 268 | 74.39 | 193.61 | 268 | 90.85 | 177.15 | 268 | 66.08 | 201.92 |

A decrease in the cutting transport velocity (Vt) can have a detrimental impact on the overall drilling process. This reduction in Vt can lead to several adverse consequences, including Cuttings Buildup, Formation Damage and Increased Drilling Fluid Consumption. As shown in Table 4, the percentage reduction in cutting transport velocity varies depending on the rock types: as 8.6% reduction in Claystone, 8.3% reduction in sand stone and 7.8% reduction in Siltstone compared to unaffected areas.

A thorough analysis, including detailed calculations involving the concentration and volume of cuttings within the affected zones, has been meticulously documented in Table 5. It is crucial to acknowledge that these zones exhibit distinct variations in rock composition. Upon obtaining these calculated values, they were subsequently use to determine the concentration of harmful elements present within the cuttings. These elements tend to accumulate within drilling fluids, giving rise to what is commonly known as waste material. This dataset serves as the primary foundation for the subsequent examination and interpretation of the element concentration ratios. Notably, the volume of cuttings within the impacted area constitutes a substantial portion, accounting for approximately 93% of the total damaged area.

**Table 5** Cutting concentration and volume in the affected interval

| Top | Base | Lithology | BTD TIME (Hrs) | Cutting Concentration Ca% | Cutting Volume Vc ($m^3$) | Average ROP (Ft/Hr) | Length of interval (m) | Time(Hr) | Cutting Volume Vc (BBL) |
|---|---|---|---|---|---|---|---|---|---|
| 2773 | 2779 | CLYST | 0 | 0.0025 | 0.33 | 1.3 | 19.68 | 15.14 | 6.4944 |
| 2779 | 2780 | SANDSTONE | 0.2 | 0.00275 | 0.22 | 1.5 | 3.28 | 2.19 | 0.7216 |
| 2780 | 2784 | CLYST | 0.6 | 0.0021 | 0.39 | 3.35 | 13.12 | 3.92 | 5.1168 |
| 2784 | 2786 | SANDSTONE | 0.9 | 0.00268 | 0.37 | 3.8 | 6.56 | 1.73 | 2.4272 |
| 2786 | 2789 | CLYST | 1.4 | 0.0019 | 0.26 | 3.03 | 9.84 | 3.25 | 2.5584 |
| 2789 | 2791 | SILTSTONE | 2 | 0.00243 | 0.59 | 4.23 | 6.56 | 1.55 | 3.8704 |
| 2791 | 2802 | CLYST | 2.8 | 0.0017 | 0.73 | 5.44 | 36.08 | 6.63 | 26.3384 |
| 2802 | 2803 | SILTSTONE | 5.9 | 0.00101 | 3.32 | 13.97 | 3.28 | 0.25 | 10.8896 |
| 2803 | 2805 | CLYST | 6.7 | 0.001 | 3.4 | 12.7 | 6.56 | 0.52 | 22.304 |
| 2805 | 2806 | SILTSTONE | 7.1 | 0.0008 | 1.85 | 8.53 | 3.28 | 0.39 | 6.068 |
| 2806 | 2808 | CLYST | 8.3 | 0.0005 | 1.48 | 5.61 | 6.56 | 1.17 | 9.7088 |
| 2808 | 2809 | SANDSTONE | 9.6 | 0.0005 | 0.75 | 4.13 | 3.28 | 0.79 | 2.46 |
| 2809 | 2811 | CLYST | 10.5 | 0.0006 | 1.46 | 4.85 | 6.56 | 1.35 | 9.5776 |
| 2811 | 2813 | SANDSTONE | 11.3 | 0.0023 | 5.14 | 20.63 | 6.56 | 0.32 | 33.7184 |
| 2813 | 2814 | SILTSTONE | 11.5 | 0.0029 | 6.29 | 31.85 | 3.28 | 0.11 | 20.6312 |
| 2814 | 2822 | CLYST | 13.1 | 0.0012 | 2.41 | 12.63 | 26.24 | 2.08 | 63.2384 |
| 2822 | 2823 | SANDSTONE | 14.6 | 0.0023 | 5.48 | 21.18 | 3.28 | 0.16 | 17.9744 |
| 2823 | 2841 | CLYST | 16.7 | 0.0023 | 2.28 | 20.34 | 59.04 | 2.90 | 134.6112 |
| 2841 | 2857 | CLYST1 | 21 | 0.0064 | 1.3 | 16 | 52.48 | 3.28 | 68.224 |
| 2857 | 2886 | CLST1B | 29.81 | 0.00425 | 2.5 | 9.47 | 95.12 | 10.10 | 237.8 |
| 2886 | 2912 | CLYST | 41.74 | 0.0018 | 1.35 | 9.02 | 85.28 | 9.46 | 115.128 |
|  |  |  |  |  |  |  |  | Sum | 799.86 |

Furthermore, in the context of total cutting volume, it is essential to acknowledge the presence of chemical element concentrations within these cuttings. These elements have been incorporated into water-based drilling fluids, ultimately resulting in environmental repercussions in the surrounding area. This impact extends not only to the natural environment but also poses potential risks to the local population residing in the region. To delve deeper into these findings and their far-reaching implications, Fig. 12 below offers detailed visual representations and analyses. This figure serves as a valuable resource for comprehending the scope and consequences of chemical element concentrations within cuttings, shedding light on their effects on the affected environment and community.

## Waste management

This study encompasses an extensive array of parameters critical for analysis, along with specific guidelines to navigate this comprehensive investigation. With the exception of parameters enclosed in parentheses, data for all other parameters were readily available for examination. These parameters underwent thorough analysis, encompassing both water and soil samples, and were reported in milligrams or micrograms per liter (mg/L or µg/L) for the dissolved phase and in parts per million (ppm) for the solid phase. Additionally, the mud-water itself was subjected to analysis similar to that of soil samples, as exemplified in Tables 6 and 7. Moreover, the investigation extended to the collection of cutting samples extracted from the well, complemented by relevant logging data. The primary objective of this phase was to determine the concentration levels of the most hazardous elements that intermingled with the drilling fluid. Of paramount importance is assessing the magnitude of their impact on the environment, particularly surface and subsurface water systems. This multi-faceted analysis represents a crucial step in comprehending the potential repercussions of drilling operations on the surrounding ecosystem and aquifers.

To conduct a comprehensive examination of the data presented in Tables 6 and 7, which detail the volume of drilling fluid retained within the cuttings, a visual representation of this information has been thoughtfully included in Fig. 13. The basis for this evaluation is the comparison framework established by the Sudanese Ministry of Oil and Gas. Through this comparative analysis, this study seeks to assess the degree to which these elements conform to the regulatory standards set by the Ministry.

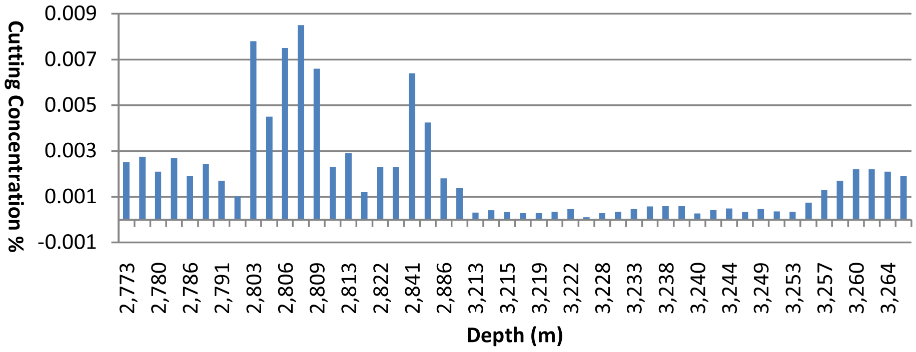

**Fig. 12** Cutting concentration%

**Table 6** Mud retention as waste in cuttings pits chemical analysis

| Parameter | | Ca | Mg | Na | K | Sr | Pb | Ni | Cu | Hg | Zn | As | Cd | Cr |
|---|---|---|---|---|---|---|---|---|---|---|---|---|---|---|
| **Unit** | | **ppm** | **ppm** | **ppm** | **ppm** | **ppm** | **ppm** | **ppm** | **ppm** | **ppm** | **ppm** | **ppm** | **ppm** | **Ppm** |
| **Locations** | 1 | 9.4 | 1468 | 11.5 | 13.1 | 424.6 | < 0.100 | 8.982 | 20.96 | | 44.97 | | 0.599 | 56.89 |
| | 2 | | | | | 94.84 | 8.82 | 102.69 | 41.63 | < LOD | 57.36 | < LOD | | |
| | 3 | 19.2 | 426.4 | 26.1 | 23.5 | 441.1 | < 0.100 | 5.788 | | | 33.39 | | 0.798 | 56.89 |
| | 4 | | | | | 59.59 | < LOD | 87.72 | < LOD | < LOD | 23.22 | < LOD | | < LOD |
| | 5 | 27.7 | 619.1 | 41.5 | 36.6 | 631.7 | < 0.100 | 96.81 | 10.18 | | 31.14 | | < 0.020 | 14.97 |
| | 6 | 9.5 | 1784 | 14.4 | 13.7 | 1552 | < 0.100 | 100.4 | 25.95 | | 76.85 | | < 0.020 | 30.54 |
| | 7 | 490 | 1018 | 1060 | 1070 | 282.4 | < 0.100 | 116.2 | 34.33 | | 36.03 | | < 0.020 | 39.72 |
| | 8 | 6371 | | | 4518.5 | 75.83 | < LOD | 40.25 | 26.47 | < LOD | 29.59 | < LOD | | < LOD |
| | 10 | 150 | 52 | 220 | 240 | 4.8 | 2.5 | 2.2 | 2.2 | | | | | |
| | 11 | | | | | 1317 | 94.12 | 1403.9 | 334.78 | 62.87 | 180.4 | 30.54 | | |
| | 12 | 3.8 | 95.15 | 7.1 | 2.2 | 3.194 | < 0.100 | < 0.100 | 2.59 | | 7.106 | | 0.599 | < 0.06 |
| | 13 | 285 | 5.344 | 1086 | 9520 | | 1.74 | < 0.100 | < 0.030 | | 0.041 | | < 0.020 | < 0.06 |
| | 14 | | | | | 74.46 | < LOD | < LOD | 26.46 | < LOD | 56.19 | < LOD | | |
| | 15 | 98.3 | 1070 | 27.8 | 24.2 | 344.3 | < 0.100 | 14.57 | 5.19 | | 17.49 | | 0.798 | 42.71 |
| | 16 | 21000 | 3700 | 1000 | 510 | 83 | 7.9 | n.a | n.a | 0.002 | | | | n.a |
| | 17 | 23133 | | | 5299.8 | 75.39 | < LOD | 109.17 | 23.32 | < LOD | 29.97 | < LOD | | < LOD |
| | 18 | 6.5 | 1686 | 11.2 | 4.7 | 484.2 | < 0.100 | 12.97 | 22.36 | | 53.77 | | 1.198 | 55.89 |
| | 19 | 1E + 05 | 2500 | 9300 | 16000 | 76 | 4.6 | n.a | n.a | | | | | n.a |
| | 20 | 2420 | | | 6519.8 | 25.36 | < LOD | 40.15 | < LOD | < LOD | 8.94 | < LOD | | < LOD |

**Table 7** Chemical analysis of solids: cuttings, mud, and soil

| Parameter | | Ca | Mg | Na | K | Sr | Pb | Ni | Cu | Hg | Zn | As | Cd | Cr |
|---|---|---|---|---|---|---|---|---|---|---|---|---|---|---|
| **Unit** | | **ppm** | **ppm** | **ppm** | **ppm** | **ppm** | **ppm** | **ppm** | **ppm** | **ppm** | **ppm** | **ppm** | **ppm** | **ppm** |
| **Locations** | 1 | 9.4 | 1468 | 11.5 | 13.1 | 424.6 | < 0.100 | 8.982 | 20.96 | | 44.97 | | 0.599 | 56.89 |
| | 2 | | | | | 94.84 | 8.82 | 102.69 | 41.63 | < LOD | 57.36 | < LOD | | |
| | 3 | 19.2 | 426.4 | 26.1 | 23.5 | 441.1 | < 0.100 | 5.788 | | | 33.39 | | 0.798 | 56.89 |
| | 4 | | | | | 59.59 | < LOD | 87.72 | < LOD | < LOD | 23.22 | < LOD | | < LOD |
| | 5 | 27.7 | 619.1 | 41.5 | 36.6 | 631.7 | < 0.100 | 96.81 | 10.18 | | 31.14 | | < 0.020 | 14.97 |
| | 6 | 9.5 | 1784 | 14.4 | 13.7 | 1552 | < 0.100 | 100.4 | 25.95 | | 76.85 | | < 0.020 | 30.54 |
| | 7 | 490 | 1018 | 1060 | 1070 | 282.4 | < 0.100 | 116.2 | 34.33 | | 36.03 | | < 0.020 | 39.72 |
| | 8 | 6371 | | | 4518 | 75.83 | < LOD | 40.25 | 26.47 | < LOD | 29.59 | < LOD | | < LOD |
| | 10 | 150 | 52 | 220 | 240 | 4.8 | 2.5 | 2.2 | 2.2 | | | | | |
| | 11 | | | | | 1316.9 | 94.12 | 1403.9 | 334.78 | 62.87 | 180.37 | 30.54 | | |
| | 12 | 3.8 | 95.15 | 7.1 | 2.2 | 3.194 | < 0.100 | < 0.100 | 2.59 | | 7.106 | | 0.599 | < 0.06 |
| | 13 | 285 | 5.344 | 1086 | 9520 | | 1.74 | < 0.100 | < 0.030 | | 0.041 | | < 0.020 | < 0.06 |
| | 14 | | | | | 74.46 | < LOD | < LOD | 26.46 | < LOD | 56.19 | < LOD | | |
| | 15 | 98.3 | 1070 | 27.8 | 24.2 | 344.3 | < 0.100 | 14.57 | 5.19 | | 17.49 | | 0.798 | 42.71 |
| | 16 | 21000 | 3700 | 1000 | 510 | 83 | 7.9 | n.a | n.a | 0.002 | | | | n.a |
| | 17 | 23133 | | | 5300 | 75.39 | < LOD | 109.17 | 23.32 | < LOD | 29.97 | < LOD | | < LOD |
| | 18 | 6.5 | 1686 | 11.2 | 4.7 | 484.2 | < 0.100 | 12.97 | 22.36 | | 53.77 | | 1.198 | 55.89 |
| | 19 | 110000 | 2500 | 9300 | 16000 | 76 | 4.6 | n.a | n.a | | | | | n.a |
| | 20 | 2420.1 | | | 6520 | 25.36 | < LOD | 40.15 | < LOD | < LOD | 8.94 | < LOD | | < LOD |

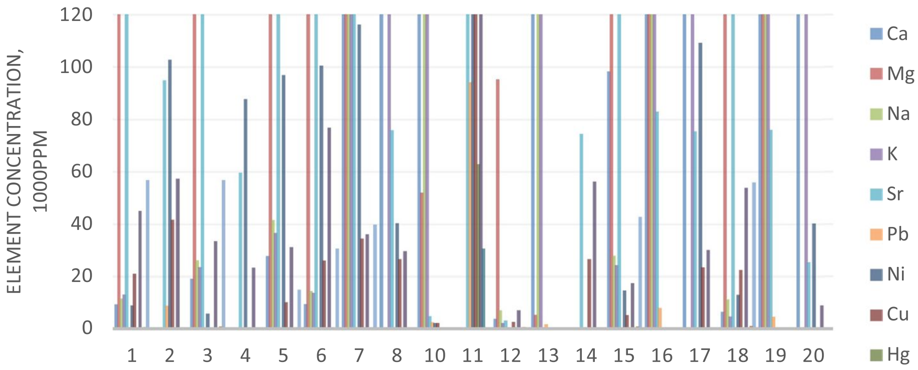

**Fig. 13** Element concentrations in mud waste from cuttings pits

The data in Table 7, which encompasses information regarding the volume of drilling cuttings, has been further elucidated through visual representations presented in Fig. 13. These graphical depictions play a pivotal role in facilitating a comprehensive comparison of the concentration levels of the most hazardous elements. This assessment holds critical importance, not only for evaluating environmental implications but also for ensuring strict compliance with safety and environmental protocols.

By conducting this analysis, the study contributes significantly to the promotion of responsible drilling practices and the maintenance of adherence to the environmental regulations established by the governing authorities. It is expected that the essential well information will be duly archived within the Ministry of Petroleum and Gas records. In cases where these data are not readily available, it is advisable to request them from the relevant operator, as detailed in Table 8.

The results obtained from the XRF screening of cutting samples strongly indicate significant contamination, with the screened concentrations notably surpassing those observed in the corresponding soil samples. An intriguing observation emerges where, despite generally lower concentrations, certain elements such as strontium (Sr), copper (Cu), and nickel (Ni) exhibit elevated values within the cuttings compared with the soil. Furthermore, analyses of the cuttings reveal heightened levels of arsenic and mercury. The presence of contamination is further underscored by inconsistent measured iron concentrations, with some duplicate samples displaying differences in up to two orders of magnitude. This emphasizes the imperative need for a thorough investigation of potential sources of contamination.

Of particular concern are the exceptionally high concentrations of calcium and potassium in the soil reference sample, raising suspicions of contamination originating from drilling mud. This specific finding accentuates the importance of handling and disposing of cuttings and mud with utmost care to mitigate environmental risks. Notably, lead (Pb), copper (Cu), and chromium (Cr) emerge as potential pollutants, demanding special attention because of their heightened presence. Moreover, surface water samples exhibit elevated concentrations of calcium and potassium, which are likely attributable to the influence of drilling mud. This reiterates the significance of exercising vigilant practices in the handling and disposal of materials.

Ultimately, the elements identified as exceeding threshold limits, including arsenic, lead, nickel, copper, and chromium, are highly probably to be contaminants present

**Table 8** Well information and inventory of drill waste

| Threshold mg/kg dry material | Excellent | Good | Moderate | Bad | Atrocious |
|---|---|---|---|---|---|
| | 🟦 | 🟩 | 🟨 | 🟥 | 🟥 |
| As | < 8 | 8-20 | 20-50 | 50-600 | 600-1000 |
| Pb | < 60 | 60-100 | 100-300 | 300-700 | 700-2500 |
| Cd | < 1.5 | 1.5-10 | 10-15 | 15-30 | 30-1000 |
| Hg | < 1 | 1-2 | 2-4 | 4-10 | 10-1000 |
| Cu | < 100 | 100-200 | 200-1000 | 1000-8500 | 8500-25000 |
| Zn | < 200 | 200-500 | 500-1000 | 1000-5000 | 5000-25000 |
| Cr+3 | < 50 | 50-200 | 200-500 | 500-2800 | 2800-25000 |
| Cr+4 | < 2 | 2-5 | 5-20 | 20-80 | 80-1000 |
| Ni | < 60 | 60-135 | 135-200 | 200-1200 | 1200-2500 |

within the cuttings. An important insight drawn from this assessment is that the most hazardous elements, according to the Ministry of Oil and Gas assessment, are heavy metals detected in both cuttings and soil. These heavy metals tend to adsorb to negatively charged mineral surfaces under near-neutral pH conditions, resulting in significantly reduced mobility compared with that of conservative ions like chloride ($Cl^{-}$), fluoride ($F^{-}$), or bromide ($Br^{-}$). This behaviour is particularly applicable to diluted concentrations of Lead ($Pb^{+2}$), Zinc ($Zn^{+2}$), Copper ($Cu^{+2}$), and Nickel ($Ni^{+2}$).

Unravelling wellbore stability and a deeper dove into data and insights, this study delves into the intricacies of wellbore stability, uncovering crucial takeaways from well log data and drilling parameters. By combining various metrics, it sheds light on factors influencing borehole integrity and paves the way for optimized drilling practices. The key findings were as follows:

- Wellbore Conditions:A combination of diverse data, including calliper measurements, bit size, and resistivity porosity, along with shear slowness data (Fig. 4), provides a comprehensive understanding of wellbore stability (Fig. 3). The equation [$\Delta t_{Shear} = 197.33e$^(-3E-06(TVD))] reveals a decreasing rate of shear slowness with increasing depth, indicating a stable and predictable formation.
- Isotropic Properties: Static Poisson's ratio, Young's modulus, and friction angle serve as brushstrokes, painting a comprehensive picture of material behaviour under stress (Fig. 5). This interplay is crucial for predicting changes in stress-laden environments, as captured by the FANG parameter ([FANG = 31.525e^(-2E-04(TVD))]). Similarly, a dedicated parameter, α, unveils rock compressibility, offering insights into pressure responses (Fig. 6, [α = 5e^(-05(TVD) + 0.169)]). Figures 7 and 8 quantify the strain–stress relationship through $v_{sta}$ and $E_{sta}$ ([$v_{sta} = 0.3149e$^(-6E-07(TVD))] and [$E_{sta} = e$^(0.0023(TVD))]), enabling the prediction of material behaviour under varying conditions.
- Safe Mud Weight Window: Pore pressure and fracture gradients (Fig. 9), estimated via well logs and Terzaghi's law, define the safe mud weight window crucial for drilling success. Analysing how wellbore stresses respond to Equivalent Circulating Density (ECD) variations (Fig. 10) further optimizes this selection. Figure 11 highlights the impact of mud weight on wellbore damage, emphasizing the significance of effective mud management.
- Drilling Fluid Performance: The stark differences in drilling fluid behaviour between the stable and unstable zones (Tables 1 and 2) are a direct consequence of contaminant intrusion. These contaminants significantly alter the fluid viscosity and yield point, impacting both cuttings transport and wellbore stability. The alarmingly high cuttings concentrations observed in unstable areas (Table 5) are a stark testament to this disruption, hinting at potential formation damage and a surge in drilling fluid consumption. Tables 3 and 4 offer detailed calculations of slip and transport velocities, revealing the intricate interplay between fluid flow and particle movement, which is crucial for understanding and mitigating these detrimental effects.
- Drilling Operation and Performance Optimization: To gain deeper insights into fluid flow and particle movement, the study calculated slip and transport veloci-

ties, revealing a potential challenge: decreased cutting transport velocity in both stable and unstable zones. This suggests broader drilling efficiency concerns that warrant further investigation. In addition, the study analysed the concentration and volume of cuttings, highlighting a significant accumulation in unstable zones. This observation provides crucial clues regarding the cause-and-effect relationship between drilling fluid behaviour and formation stability.

## Conclusions

- Precise data analysis pinpointed a critical instability in Rawat Field, where wellbore collapse correlated with low mud density (10 ppg) and specific formation characteristics. The optimal mud density for stable drilling lies within the 13.5–15.5 ppg range.
- Unexpectedly, the extracted cuttings far exceeded the water-based mud expectations, revealing significant mud waste (>800 BBL). This raises environmental concerns due to high levels of harmful elements (lead, mercury, nickel, etc.) in the waste, posing risks to groundwater and agriculture.
- Therefore, we urge the implementation of scientifically sound waste management strategies. Sludge separation, treatment, and proper disposal are crucial to mitigate the environmental impact. Embracing sustainable drilling practices, advanced technologies, and effective waste management is essential for protecting groundwater and agricultural resources (see Fig. 14).
- Proper mud waste management is an environmental imperative, safeguards groundwater and promotes sustainable agricultural practices. New technologies in drilling methods and waste treatment are key to minimizing environmental impacts.

## Recommendation

The oil and gas industry faces the daunting challenges of wellbore instability and formation damage, particularly in complex geological environments such as depleted fields and deepwater settings. This highlighted several advancements in drilling and completion technologies that offer promising solutions to these issues. Further advancements in data analytics, machine learning, and geomechanical modelling are expected to refine these technologies and provide even more effective solutions for drilling in mature oil and gas fields. By adopting these innovative approaches, the industry can tackle wellbore instability and formation damage with greater precision and efficiency, maximizing hydrocarbon recovery and minimizing environmental impact. Here are some:

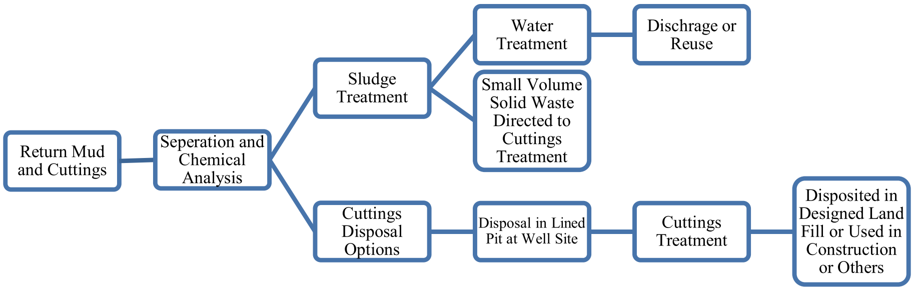

**Fig. 14** Proposed waste management and treatment system

1. Conduct Comprehensive Research on Chemical Element Concentration: It is essential to conduct thorough and extensive research to investigate the concentration of chemical elements within sedimentary rocks. Such research endeavours can provide invaluable insights into the potential environmental impacts and safety considerations associated with drilling and extraction processes. This knowledge will help make informed decisions and implementing appropriate measures to mitigate risks.
2. Adhere to Rigorous Safety Standards and Scientific Waste Treatment: Companies operating in the oil industry should steadfastly adhere to established safety standards and procedures. Furthermore, they must recognize the critical importance of employing scientific methods for treating waste materials resulting from their activities. This proactive approach is indispensable for mitigating environmental damage, safeguarding the plant sector, and preserving water resources.
3. Implement Geomechanical Assessments as Standard Practice: It is advisable to incorporate geomechanical assessments as a standard practice before starting any drilling or operational activities. Thorough geomechanical evaluations can effectively identify and proactively address potential risks and challenges. This approach not only enhances operational safety but also contributes to the efficient and responsible use of geological resources.
4. Establish Dedicated Rock Mechanical Laboratories in Educational Institutions: A vital recommendation is the creation of dedicated rock mechanical laboratories within educational institutions, particularly universities. Such facilities can serve as educational hubs, fostering an understanding of geomechanical models and their practical applications. This initiative can significantly contribute to the development of a skilled workforce equipped with the knowledge and tools necessary for sustainable resource management.

These recommendations promote responsible and sustainable practices within the drilling industry while minimizing negative impacts on the environment and local communities.

**Abbreviations**

| | |
|---|---|
| TVD | Is the True Vertical Depth, m |
| $V_{sh}$ | Is the volume of shale, g/cm$^3$ |
| GR | Is the gamma-ray measurement value |
| $GR_{index}$ | Is the gamma-ray index calculated during the process |
| $GR_{matrix}$ | Represents the gamma-ray measurement from the matrix |
| $GR_{shale}$ | Represents the gamma-ray measurement from the shale |
| ØT | Represents the total porosity, PU |
| ØE | Signifies the effective porosity, PU |
| $ØT_{sh}$ | Denotes the total shale porosity, PU |
| $\rho_{ma}$ | Is the matrix density, g/cm$^3$ |
| $\rho_B$ | Is the bulk density, g/cm$^3$ |
| $\rho_f$ | Is the formation fluid density, g/cm$^3$ |
| $\rho_{sh}$ | Is the shale density, g/cm$^3$ |
| $\rho_{AMOCO}$ | Is the average formation bulk density under the sea floor, g/cm$^3$ |
| $A_0$ | Is a constant factor |
| $(\propto)$ | Alpha is a constant exponent in the equation, set at 0.6 |
| $P_P$ | Represents the predicted pore pressure, psi |
| $\sigma_v$ | Denotes the sonic velocity, m/s |
| $PP_{norm}$ | Represents the reference or baseline pore pressure value, psi |
| $\alpha$ | Is a constant Biot factor |
| $R/R_{norm}$ | Is the ratio of the formation density to the reference or baseline density |

| | |
|---|---|
| Z | Is the depth measured from the sea floor, m |
| R | Is the measurement factor value |
| $R_o$ | Is the measurement factor value at the sea floor |
| $R_{norm}$ | Is the measurement factor value if the formation was normally pressured |
| $P_{norm}$ | Is the normal pore pressure, psi |
| a and n | Are fitting parameters called the Eaton factor and Eaton exponent, respectively, and the default values for the Eaton method are as follows: ✓ a = 1, ✓ n = 3 (compressional slowness); and n = 1.2 (resistivity or d-exponent) |
| FG | Represents the fracture gradient, psi/m |
| K | Signifies the stress ratio, a dimensionless parameter that is calculated as the horizontal effective matrix stress divided by the effective vertical stress |
| $\sigma_v$ | Denotes the vertical effective stress, lb/in2 |
| $K_{dyn}$ | Represents the dynamic bulk modulus |
| $\Delta t_{comp}$ | Signifies the compressive slowness |
| $G_{dyn}$ | Stands for dynamic shear modulus |
| $\Delta t_{Shear}$ | Signifies the shear slowness |
| $E_{dyn}$ | Denotes the dynamic Young's modulus |
| $V_{dyn}$ | Signifies the dynamic Poisson ratio |
| $R_{sp}$ | Represents the ratio of shear to compressional slowness |
| $\Delta t_{Shear}$^2 and $\Delta t_{comp}$^2 | represent the square of shear and compressional slowness, respectively |
| $E_{sta}$ | Represents the static Young's modulus |
| $v_{sta}$ | Signifies static Poisson's ratio |
| $C_0$ | Represents the Coates Denoo Correlation constant factor |

**Acknowledgements**
This paper is the product of a collaborative effort between the Ministry of Energy and the Petroleum Department of Sudan University of Science and Technology. The author extends his sincere appreciation to both institutions for their trust and support in facilitating this research.

**Authors' contributions**
As the corresponding author, I performed a thorough analysis and interpretation of the data presented in the research titled "Enhancing Drilling Operations: Prioritizing Wellbore Integrity, Formation Preservation, and Effective Mud Waste Control (Case Study)." I hereby confirm my endorsement of this manuscript and its contents. Furthermore, I assume the role of overseeing the peer review process and ensuring strict adherence to the transparency and reproducibility standards specific to our field and the journal. This encompasses safeguarding the integrity of the original data, validating the accuracy of information representation, and advocating for data sharing.

**Funding**
Not applicable.

**Availability of data and materials**
The study's supporting data can be obtained from the [Ministry of Energy—Sudan]. However, there are restrictions on public access to these data because they were used under a licensing agreement for this specific research. Nonetheless, the authors are willing to provide the data upon a reasonable request, subject to approval from the [Energy Ministry—Sudan].

## Declarations

**Competing interests**
The authors declare that they have no competing interests.

Received: 2 October 2023 Accepted: 2 February 2024

**References**
1. Abbas KM, Hossein J, Masoud A (2014) Analysis of vertical, horizontal and deviated wellbores stability by analytical and numerical methods. J Pet Explor Prod Technol 4(4):359369. https://doi.org/10.1007/s13202-014-0100-7
2. Ibrahim AA, Hassan HI, Musa TA (2019) Analyses of formation damage caused by drilling fluid. Alsalam Univ J 3(7). http://alsalam.edu.sd/journal/index.php/suj/article/view/63. Khartoum, Sudan
3. Civen F (2000) Reservoir formation damage, modeling, assessment, and mitigation, 2nd edn. Gulf Publishing Company Houston, Texas. Index. ISBN 0-88415-301-0
4. McLean MR, Addis MA (1990) Wellbore stability analysis: a review of current methods of analysis and their field application. Paper presented at the IADC/SPE Drilling Conference, Houston. https://doi.org/10.2118/19941-MS
5. Mclenllan P, Hawkes C (2001) Borehole stability analysis for underbalanced drilling analysis of wellbore instability in vertical, directional, and horizontal wells using field data. J Can Petr Technol 40(5):31–38. https://doi.org/10.2118/01-05-01
6. He S, Wang W, Shen H, Tang M, Liang H, Lu J (2015) Factors influencing wellbore stability during underbalanced drilling of horizontal wells when fluid seepage is considered. J Nat Gas Sci Eng 23:80–89. https://doi.org/10.1016/j.jngse.201501029

7. Aradhi KK, Dasari BM, Banothu D, Manavalan S (2023) Spatial distribution, sources and health risk assessment of heavy metals in topsoil around oil and natural gas drilling sites, Andhra Pradesh, India. Sci Rep 13(1):10614. https://doi.org/10.1038/s41598-023-36580-9. PMID:37391457; PMCID: PMC10313719
8. KhodoliZangeneh D, Amanipoor H, Battaleb-Looie S (2023) Evaluation of heavy metal contamination using cokriging geostatistical method (Case study of Abteymour Oilfield in Southern Iran). Appl Water Sci J 13:200. https://doi.org/10.1007/s13201-023-01980-9
9. Ndufor PN, Idehen KI (2005) Environmental impact of oil and gas operation: a case study of drilling-mud disposal in Niger Delta, Nigeria. Paper presented at the SPE/EPA/DOE Exploration and Production Environmental Conference, Galveston. https://doi.org/10.2118/94291-MS
10. Onwugbuta N, Ekweozor IKE, Ugbomeh AP, Anaero-Nweke GN, Bobmanuel KNO (2022) Assessment of heavy metals in soils and manihot esculenta of some selected communities in Niger Delta. Int J Adv Res Biol Sci 9(12):74–96. https://doi.org/10.22192/ijarbs.2022.09.12.007
11. Ekpete OA, Edori OS, Iyama WA (2019) Concentrations of polycyclic aromatic hydrocarbons from selected dumpsites within port Harcourt metropolis, Rivers State, Niger Delta, Nigeria. Int J Environ Sci Nat Res 21(4):556066. https://doi.org/10.19080/IJESNR.2019.21.556066
12. Ekpo BO, Oyo-Ita OE, Oros DR, Simoneit BR (2012) Distributions and sources of polycyclic aromatic hydrocarbons in surface sediments from the cross river estuary, S. E. Niger Delta, Nigeria. Environ Monit Assess 184(2):1037–47. https://doi.org/10.1007/s10661-011-2019-5
13. Iwegbue CMA, Irerhievwie GO, Tesi GO, Olisah C, Nwajei GE, Martincigh BS (2021) Polycyclic Aromatic Hydrocarbons (PAHs) in surficial sediments from selected rivers in the Western Niger Delta of Nigeria: spatial distribution, sources, and ecological and human health risks. Mar Pollut Bull 67:112351. https://doi.org/10.1016/j.marpolbul.2021.112351
14. Anyanwu IN, Beggel S, Sikoki FD et al (2023) Pollution of the niger delta with total petroleum hydrocarbons, heavy metals and nutrients in relation to seasonal dynamics. Sci Rep 13:14079. https://doi.org/10.1038/s41598-023-40995-9
15. Oyibo JN, Wegwu MO, Uwakwe AA, Osuoha JO (2018) Analysis of total petroleum hydrocarbons, polycyclic aromatic hydrocarbons and risk assessment of heavy metals in some selected finfishes at forcados terminal, Delta State, Nigeria. Environ Nanotechnol Monitor Manag 9:128–13. https://doi.org/10.1016/j.enmm.2017.11.002
16. Yang Z, Wang Z, Yang C, Hollebone BP, Brown C, Landriault M (2013) Evaluation of Total Petroleum Hydrocarbons (TPH) measurement methods for assessing oil contamination in soil. Environ Forensics 14:193–203. https://doi.org/10.1080/15275922.2013.814180
17. Guo J, Chen W, Wu M, Qu C, Sun H, Guo J (2023) Distribution, sources, and risk assessment of organochlorine pesticides in water from Beiluo River, Loess Plateau, China. Toxics 11(6):496. https://doi.org/10.3390/toxics11060496
18. Okoffo ED, Darko G, Gordon C (2016) Assessment of organochlorine pesticide residues in soils and drinking water sources from cocoa farms in Ghana. SpringerPlus 5(1):1–13. https://doi.org/10.1186/s40064-016-2352-9
19. Olisah C, Okoh OO, Okoh AI (2020) Occurrence of organochlorine pesticide residues in biological and environmental matrices in africa: a two-decade review. Heliyon 6(3):e03518. https://doi.org/10.1016/j.heliyon.2020.e03518
20. Radwan AE, Wood DA, Abudeif AM et al (2022) Reservoir formation damage; reasons and mitigation: a case study of the cambrian-ordovician nubian 'C' sandstone gas and oil reservoir from the gulf of suez rift basin. Arab J Sci Eng 47:11279–11296. https://doi.org/10.1007/s13369-021-06005-8
21. Radwan AE (2021) Integrated reservoir, geology, and production data for reservoir damage analysis: a case study of the miocene sandstone reservoir, Gulf of Suez, Egypt. Interpretation 9(4):27–37. https://doi.org/10.1190/INT-2021-0039.1
22. Zhao X, Qiu Z, Sun B, Liu S, Xing X, Wang M (2019) Formation damage mechanisms associated with drilling and completion fluids for deepwater reservoirs. J Petrol Sci Eng 173:112–121. https://doi.org/10.1016/j.petrol.2018.09.098
23. Gamal H, Elkatatny S (2022) The impact of overbalance pressure on the alteration of sandstone geomechanical properties. J Pet Explor Prod Technol 13(1):1–11. https://doi.org/10.1007/s13202-022-01540-y
24. Zhang F, Liu HB, Cui S, Meng YF, Wang JJ (2021) Influence of the weakening effect of drilling fluid on wellbore stability in anisotropic shale formation. Front Phys 9:745075. https://doi.org/10.3389/fphy.2021.745075
25. Halim MC, Hamidi H, Akisanya AR (2022) Minimizing formation damage in drilling operations: a critical point for optimizing productivity in sandstone reservoirs intercalated with clay. Energies 15(1):162. https://doi.org/10.3390/en15010162
26. Liu H, Cui S, Meng Y, Fan Y, Liu T, Yu A, Hu Z (2020) Wellbore stability evaluation method based on the continuous tangent envelope of a mohr circle. Sci Prog 103(1):0036850419888465. https://doi.org/10.1177/0036850419888465
27. Gholami R, Rabiei M, Aadnoy B, Rasouli V (2018) A methodology for wellbore stability analysis of drilling into presalt formations: a case study from Southern Iran". J Pet Sci Eng 167:249–261. https://doi.org/10.1016/j.petrol.2017.11.023
28. Elemam AE, Hussien RAM, Ibrahim AA, Mohamed SA (2017) Impacts of Polyanionic Cellulose Polymer (PAC-LV) on drilling fluids properties. SUST J Eng Comput Sci 18(3). Khartoum, Sudan
29. Ibrahim AA, Musa TA, AiGou Y (2001) Application study of bit selection, bit weight and rotary speed in Sudan. In: Published in the proceedings of applications and development of geo-drilling and tunnelling technology in resource, environmental and construction Conference, p 198–201
30. Eren T, Ozbayoglu ME (2010) Real time optimization of drilling parameters during drilling operations. Paper presented at the SPE Oil and Gas India Conference and Exhibition, Mumbai. https://doi.org/10.2118/129126-MS
31. Ahmed SS, Ibrahim AA (2020) Overcoming the data limitation that restrict drilling optimization across multiple regression approach. Elixir Int J Pet Eng 141(4):54280–54289
32. Ahmed SS, Ibrahim AA (2019) Bourgoyne and young model development review. Int J Eng Sci Technol 8(6):164–174. https://doi.org/10.5281/zenodo.3256067
33. Sui D, Nybø R, Azizi V (2013) Real-time optimization of rate of penetration during drilling operation. In: 10th IEEE International Conference on Control and Automation (ICCA), Hangzhou, p 357-362. https://doi.org/10.1109/ICCA.2013.6564893
34. Abbas AK (2021) Experimental investigation of cuttings transport with nanocomposite water-based drilling fluids modified by cellulose nanoparticles. Colloids Surf A 615:126240. https://doi.org/10.1016/j.colsurfa.2021.126240

35. Ibrahim AA, Musa TA (2003) Experimental study optimizing hole cleaning-cutting transport in oil drilling engineering. China Univ Geosci J 14(2):182–189. Whan, China
36. An J, Li J, Huang H, Liu G, Yang H, Zhang G, Chen S (2023) Transient cutting transport model for horizontal wells with a slim hole. Energy Sci Eng 11(2):796–810. https://doi.org/10.1002/ese3.1363
37. Erge O, Ozbayoglu EM, Miska SZ, Yu M, Takach N, Saasen A, May R (2015) Laminar to turbulent transition of yield power law fluids in annuli. J Petrol Sci Eng 128:128–139. https://doi.org/10.1016/j.petrol.2015.02.007
38. Güzel B, Burghelea T, Frigaard I, Martinez D (2009) Observation of laminar-turbulent transition of a yield stress fluid in hagen-poiseuille flow. J Fluid Mechan 627:97–128. https://doi.org/10.1017/S0022112009005813
39. Katende A, Segar B, Ismail I, et. al. (2020) The effect of drill-pipe rotation on improving hole cleaning using polypropylene beads in water-based mud at different hole angles. J Petrol Explor Prod Technol 10:1253–1262. https://doi.org/10.1007/s13202-019-00815-1
40. Reed TD, Pilehvari AA (1993) A new model for laminar, transitional, and turbulent flow of drilling muds. Paper presented at the SPE Production Operations Symposium, Oklahoma City. https://doi.org/10.2118/25456-MS
41. Elrayah AAI, Hussein AAF (2017) Pore pressure regime for Bentiu-1 formation, Sudan. Red Sea Univ J Basic Appl Sci 2(2). Sudan
42. Chen G, Chenevert ME, Sharma MM, Yu M (2003) Wellbore stability in shales including poroelastic, chemical, and thermal effects. J Petr Sci Eng 38(3):167–176. https://doi.org/10.1016/S0920-4105(03)00030-5
43. Yeu WJ, Katende A, Sagala F, Ismail I (2018) Improving hole cleaning using low density polyethylene beads at different mud circulation rates in different hole angles. J Nat Gas Sci Eng 61:333–343. https://doi.org/10.1016/j.jngse.2018.11.012
44. Radwan AE (2022) Drilling in complex pore pressure regimes: analysis of wellbore stability applying the depth of failure approach. Engineers 15(21):7872. https://doi.org/10.3390/en15217872. Kraków, Poland
45. Campa MF, Wolfe AK, Techtmann SM, Harik A, Hazen TC (2019) Unconventional oil and gas energy systems: an unidentified hotspot of antimicrobial resistance. Front Microbiol 10:472509
46. Grillitsch B, Gans O, Kreuzinger N, Scharf S, Uhl M, Fuerhacker M (2006) Environmental risk assessment for quaternary ammonium compounds: a case study from Austria. Water Sci Technol 54(11–12):111–8. https://doi.org/10.2166/wst.2006.840. PMID:17302311
47. Shi X, Zhang R, Sand W, Mathivanan K, Zhang Y, Wang N, Duan J, Hou B (2023) Comprehensive review on the use of biocides in microbiologically influenced corrosion. Microorganisms 11(9):2194. https://doi.org/10.3390/microorganisms11092194
48. Uche OMD, Ismail IB, Piroozian A, Mamat NS, Ismail ASI (2015) Improving the cuttings transport performance of water-based mud through the use of polypropylene beads. Sains Malays 44:629–634

## Publisher's Note